PLANT SCIENCE

Morphinan biosynthesis in opium poppy requires a P450-oxidoreductase fusion protein

Thilo Winzer,[1] Marcelo Kern,[1] Andrew J. King,[1] Tony R. Larson,[1] Roxana I. Teodor,[1] Samantha L. Donninger,[1] Yi Li,[1] Adam A. Dowle,[2] Jared Cartwright,[2] Rachel Bates,[2] David Ashford,[2] Jerry Thomas,[2] Carol Walker,[3] Tim A. Bowser,[3] Ian A. Graham[1]*

Morphinan alkaloids from the opium poppy are used for pain relief. The direction of metabolites to morphinan biosynthesis requires isomerization of (*S*)- to (*R*)-reticuline. Characterization of high-reticuline poppy mutants revealed a genetic locus, designated *STORR* [*(S)- to (R)-reticuline*] that encodes both cytochrome P450 and oxidoreductase modules, the latter belonging to the aldo-keto reductase family. Metabolite analysis of mutant alleles and heterologous expression demonstrate that the P450 module is responsible for the conversion of (*S*)-reticuline to 1,2-dehydroreticuline, whereas the oxidoreductase module converts 1,2-dehydroreticuline to (*R*)-reticuline rather than functioning as a P450 redox partner. Proteomic analysis confirmed that these two modules are contained on a single polypeptide in vivo. This modular assembly implies a selection pressure favoring substrate channeling. The fusion protein STORR may enable microbial-based morphinan production.

The naturally occurring opiates of the morphinan subclass of benzylisoquinoline alkaloids (BIAs) include morphine, codeine, and thebaine. Morphine and codeine can be directly used as analgesic painkillers, and thebaine is widely used as a feedstock for the synthesis of a number of semisynthetic opiates, including hydrocodone, hydromorphone, oxycodone, and oxymorphone, as well as the opioid antagonist naloxone. The discovery and isolation of morphine from the opium poppy (*Papaver somniferum* L.) by Friedrich Sertürner in 1806 (*1*) are a milestone in the history of pharmacy. More than 200 years later, opiate alkaloid–based pharmaceutical formulations remain the most potent treatment for severe pain, with sales totaling $US11.6 billion in 2013 (*2*).

BIAs are found in a number of species in the Papaveraceae family, but morphine production has only been reported in the opium poppy and the closely related *P. setigerum* (*3*). The morphinan backbone contains five asymmetric carbon centers. Total chemical synthesis, although possible (*4*), is not an economically viable means of production. Consequently, morphinan alkaloids are still exclusively sourced from the opium poppy plant. Much effort has gone into the elucidation of the morphinan branch of BIA metabolism over the past 25 years, resulting in the identification of genes for all but the gateway step involving the epimerization of (*S*)- to (*R*)-reticuline (*3*, *5*–*14*). Thus, although it has been possible to produce both (*S*)- and racemic mixtures of (*R*,*S*)-reticuline and morphinans in metabolically engineered microbial systems (*15*–*18*), the clean enzymatic conversion of (*S*)- to (*R*)-reticuline remains the goal.

(*S*)-reticuline is the central intermediate of BIA metabolism (fig. S1), and conversion to its R epimer is believed to be a two-step process (*19*, *20*). The S epimer is first oxidized to the quaternary positively charged amine 1,2-dehydroreticuline, followed by reduction to (*R*)-reticuline (Fig. 1A). Activities for each step have been reported, but the identity of the corresponding proteins has not been established (*19*, *20*). We have combined a candidate gene approach with genetic analyses of F_2 populations of *P. somniferum* segregating for mutations that are deficient in (*S*)- to (*R*)-reticuline conversion and discovered that a fusion protein is responsible for sequentially catalyzing both steps of the epimerization.

RNA interference (RNAi) knockdown of codeinone reductase in the opium poppy was reported to cause accumulation of (*S*)-reticuline, which is eight steps upstream of the codeinone reductase substrate (*21*), a result the authors attributed to metabolite channeling. We considered an alternative hypothesis to be the off-target cosilencing of a closely related oxidoreductase involved in the conversion of (*S*)- to (*R*)-reticuline. Using the sequence of the RNAi silencing construct to query an in-house expressed sequence tag (EST) library from stem and capsule tissue of opium poppies (*22*), we identified a contiguous assembly comprising a cytochrome P450 monooxygenase that is 3′-linked to an oxidoreductase. Sequencing cDNA clones from opium poppy stems confirmed the in-frame fusion transcript (Fig. 1A and fig. S2). The P450 module was designated CYP82Y2.

To investigate whether the corresponding gene is a candidate for one or both steps in the epimerization of (*S*)- to (*R*)-reticuline, we sequenced corresponding cDNA clones from three independent mutants identified from an ethyl methanesulfonate–mutagenized population of a high-morphine cultivar, HM2 (*23*). All three mutants have lost the ability to produce morphinan alkaloids and instead accumulate high levels of (*S*)-reticuline as well as the (*S*)-reticuline–derived alkaloids laudanine and laudanosine (Fig. 1, B and D). We found that all three mutant lines carry mutations in the corresponding gene locus (Fig. 1A), which we name *STORR* [*(S)- to (R)-reticuline*]. The *storr-1* allele carries a premature stop codon corresponding to amino acid position W668 in the oxidoreductase module of the predicted fusion protein. *storr-1* plants also contain low but significant levels of 1,2-dehydroreticuline (Fig. 1C), which suggests that the oxidoreductase module catalyzes the second step of the epimerization, the reduction of 1,2-dehydroreticuline to (*R*)-reticuline. *storr-2* and *storr-3* are both disrupted in the CYP82Y2 module: *storr-2* contains a premature stop at codon position W278, and *storr-3* contains a missense mutation causing a glycine-to-arginine substitution at position 550 (Fig. 1A). Dried capsules of *storr-2* and *storr-3* accumulate (*S*)-reticuline but not 1,2-dehydroreticuline, suggesting that the CYP82Y2 module is responsible for the first epimerization step, the oxidation of (*S*)-reticuline to 1,2-dehydroreticuline. Complementation tests and F_2 segregation analysis confirmed that a single genetic locus is responsible for the high-reticuline phenotype, association of the three recessive *storr* alleles with the high-reticuline phenotype, and the consecutive roles of the CYP82Y2 and oxidoreductase modules in the epimerization of (*S*)- to (*R*)-reticuline (tables S2 and S3).

To establish whether the *STORR* locus is not only transcribed but also translated as a fusion protein, we used a quantitative mass spectrometry approach after gel fractionation of crude protein extract from HM2. Peptides from across the entire STORR protein were found to be most abundant in the gel regions covering the 100.65-kD predicted size of the fusion protein, confirming this as the in vivo form (Fig. 2). For direct functional characterization, the STORR fusion protein and the separate modules were expressed in *Saccharomyces cerevisiae*, and enzyme assays were performed on soluble extracts and microsomal preparations (Fig. 3). We found that 1,2-dehydroreticuline is converted to (*R*)-reticuline with 100% conversion efficiency by both the STORR fusion protein and the oxidoreductase module, but not by the CYP82Y2 module plus its redox partner (Fig. 3A). In contrast, the CYP82Y2 module plus its redox partner catalyzed 97% conversion of (*S*)-reticuline to 1,2-dehydroreticuline,

[1]Centre for Novel Agricultural Products, Department of Biology, University of York, York YO10 5DD, UK. [2]Bioscience Technology Facility, Department of Biology, University of York, York YO10 5DD, UK. [3]GlaxoSmithKline, 1061 Mountain Highway, Post Office Box 168, Boronia, Victoria 3155, Australia.
*Corresponding author. E-mail: ian.graham@york.ac.uk

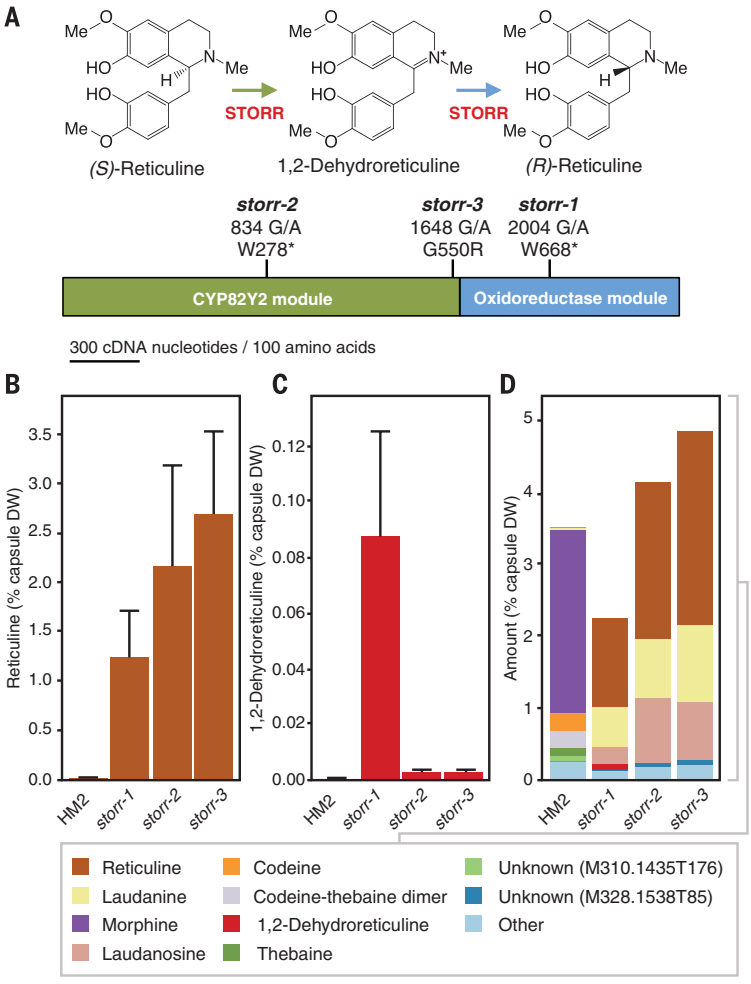

Fig. 1. Characterization of opium poppy mutants disrupted in the conversion of (*S*)- to (*R*)-reticuline. (**A**) Schematic showing epimerization of (*S*)- to (*R*)-reticuline and position of the *storr-1*, *storr-2*, and *storr-3* mutations in the predicted fusion protein. (**B**) Mean ± SD capsule reticuline content in the HM2 wild-type cultivar and *storr* mutants (HM2, $n = 5$; *storr-1*, $n = 12$; *storr-2*, $n = 17$; *storr-3*, $n = 15$). DW, dry weight. Reticuline content was verified as >99.2% (*S*)-reticuline in all mutants by chiral high-performance liquid chromatography (HPLC) (table S1). (**C**) 1,2-dehydroreticuline. (**D**) All compounds >1% total alkaloids ($n = 10$) are individually identified, with minor peaks ($n = 379$), grouped as "Other."

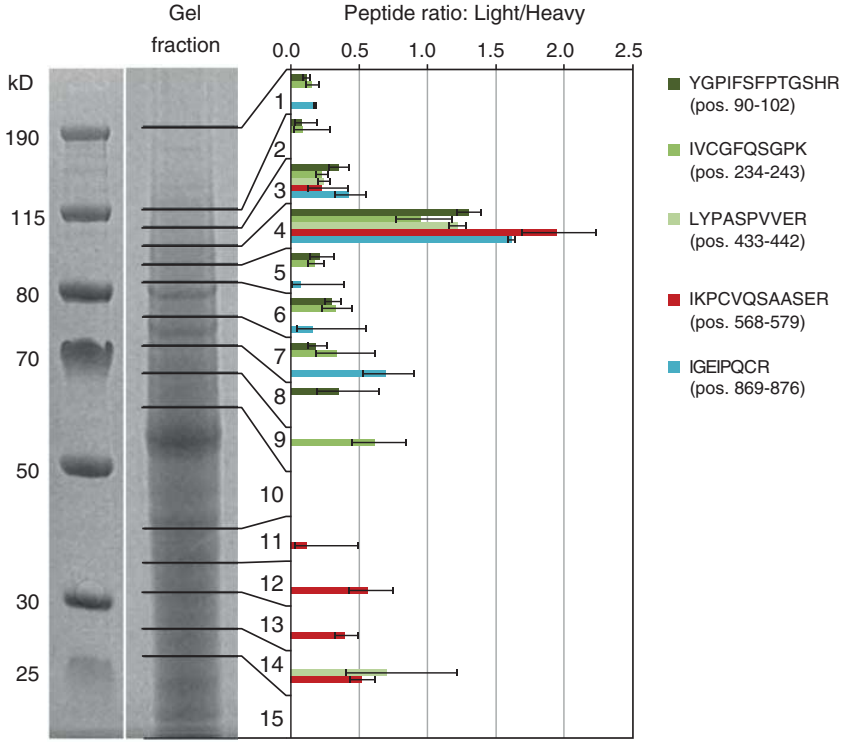

Fig. 2. Size determination of STORR protein in the opium poppy. Protein extracts from three stem samples of HM2 wild type were fractionated, together with size markers, by SDS–polyacrylamide gel electrophoresis (SDS-PAGE), and the three lanes were each cut into 15 fractions (see horizontal lines on one representative lane) to resolve the predicted fusion protein and putative individual CYP450 and oxidoreductase modules (101, 65, and 36 kD, respectively). For relative quantification, an equal amount of a tryptic digest of ^{15}N-labeled recombinant STORR protein was spiked into the in-gel digest of each SDS-PAGE fraction before HPLC mass spectrometry (HPLC-MS). Ratios of peak areas from extracted-ion chromatograms of light (endogenous) to heavy (labeled) versions of five peptides from across the STORR protein sequence were compared. Ratios of normalized peak areas from extracted-ion chromatograms were converted to binary logarithms for the calculation of means and standard errors of the mean. Only measurements where the respective peptides were found in all three biological replicates are shown.

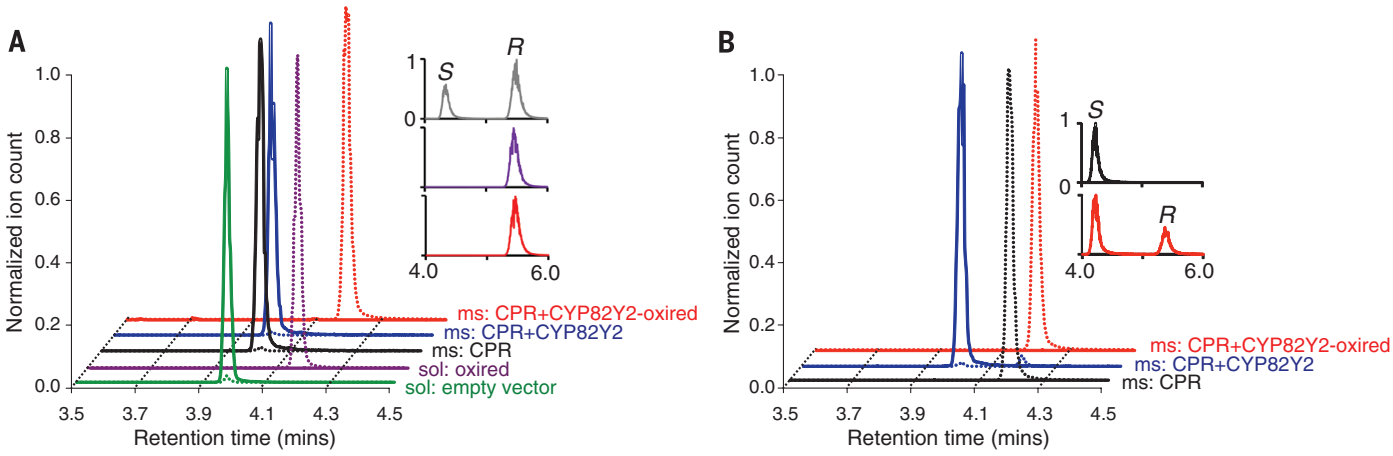

Fig. 3. Functional characterization of the STORR fusion protein by heterologous expression in *S. cerevisiae*. (**A**) HPLC-MS analysis of the in vitro conversion of 1,2-dehydroreticuline to (*R*)-reticuline. Crude soluble (sol) or microsomal (ms) preparations harboring the empty pESC-TRP vector (green), vector containing the oxidoreductase module (purple), an opium poppy cytochrome P450 reductase (CPR) redox partner (black), CPR + CYP82Y2 (blue), or CPR + the CYP82Y2-oxidoreductase fusion (red) were assayed (*21*). The solid lines of the HPLC-MS chromatograms show the normalized total ion count at a mass/charge ratio (*m/z*) of 328, corresponding to 1,2-dehydroreticuline (substrate), whereas the dotted lines show the normalized total ion count at *m/z* 330, corresponding to reticuline (product). The inset panel shows the chiral analysis of reticuline: The gray trace is for an (*S*)- and (*R*)-reticuline standard, and the purple and red traces correspond to reticuline derived by activity of the oxidoreductase and CYP82Y2-oxidoreductase fusion, respectively. (**B**) HPLC-MS analysis of the conversion of (*S*)-reticuline into 1,2-dehydroreticuline and (*R*)-reticuline. Crude microsomal preparations obtained from *S. cerevisiae* harboring expression vector pESC-TRP containing CPR only (black), CPR + a CYP82Y2 module (blue), or CPR + CYP82Y2-oxidoreductase fusion (red) were assayed (*21*). The solid lines of the HPLC-MS chromatograms show the normalized total ion count at *m/z* 328, corresponding to 1,2-dehydroreticuline, and the dotted lines show the normalized total ion count at *m/z* 330, corresponding to reticuline. The inset panel shows the chiral analysis of reticuline, with the same line colors as in the main panel.

demonstrating that it acts as a 1,2-dehydroreticuline synthase (Fig. 3B). Microsomal preparations harboring the entire STORR fusion protein converted about 20% of the added (*S*)-reticuline to (*R*)-reticuline, confirming the bifunctional role of the protein in performing sequential reactions in the epimerization of reticuline. Kinetic analysis revealed that the microsomal CYP82Y2 module alone and the CYP82Y2-oxidoreductase fusion had similar Michaelis constant values of 13 and 14 μM for (*S*)-reticuline and 1,2-dehydroreticuline, respectively (fig. S3). Consistent with the plant mutant phenotypes, we found that microsomally expressed STORR carrying the *storr-2* mutation lacks both the P450 and oxidoreductase activities, the *storr-3* mutation lacks the P450 activity but does still exhibit the oxidoreductase activity, and the *storr-1* mutation has lost the oxidoreductase activity but maintains very low levels of P450 activity (fig. S4).

P450-redox systems where the P450 enzyme is covalently linked to redox partner reductase components are well known in both prokaryotes and lower eukaryotes (*24*). In the STORR fusion protein, the P450 module is linked to a reductase, but rather than functioning as a redox partner for the P450, this reductase catalyzes the product of the P450 to complete a two-step epimerization of (*S*)- to (*R*)-reticuline. Other forms of bifunctional P450 fusions with oxygenase/peroxidase, hydrolase, and dioxygenase modules have been reported to occur in ascomycetes, and all of these also appear to catalyze sequential reactions (*25*–*27*). A possible explanation as to why such fusion proteins evolve is that they facilitate efficient channeling of highly unstable or reactive intermediates. Evidence for efficient substrate channeling in the case of the STORR fusion protein comes from the observation that microsomal fractions harboring the fusion protein directly convert (*S*)- to (*R*)-reticuline, with no detectable accumulation of 1,2-dehydroreticuline (Fig. 3B).

Phylogenetic analysis suggests that the *STORR* fusion occurred after the split of the CYP82X and the CYP82Y subfamilies and that the oxidoreductase module falls into subfamily 4 of the aldo-keto reductases, with closest homology to the codeinone reductase family from *P. somniferum* (fig. S5). A query of the 1K plant transcriptome resource (*28*) identified similar predicted module arrangements in EST collections from two other morphinan-producing *Papaver* species, *P. bracteatum* and *P. setigerum*, but not in *P. rhoeas*, which does not make morphinans (table S4). We hypothesize that the STORR fusion was the key step in the evolution of the morphinan branch of BIA metabolism. After this step, other enzymes were recruited and adapted, including dioxygenases and reductases, ultimately giving rise to codeine and morphine in *P. somniferum* and *P. setigerum* (*29*). Thus, this morphinan biosynthetic pathway, and probably other plant secondary metabolic pathways, depends on the organization of both individual gene structure and genome rearrangement (*22*).

REFERENCES AND NOTES

1. F. Sertürner, *J. Pharmacie* **14**, 47–93 (1806).
2. IMS Health Database, Formulation sales by opiate molecule, www.imshealth.com (2013).
3. J. Ziegler *et al.*, *Plant J.* **48**, 177–192 (2006).
4. M. Gates, G. Tschudi, *J. Am. Chem. Soc.* **78**, 1380–1393 (1956).
5. N. Samanani, D. K. Liscombe, P. J. Facchini, *Plant J.* **40**, 302–313 (2004).
6. A. Ounaroon, G. Decker, J. Schmidt, F. Lottspeich, T. M. Kutchan, *Plant J.* **36**, 808–819 (2003).
7. K. B. Choi, T. Morishige, F. Sato, *Phytochemistry* **56**, 649–655 (2001).
8. H. H. Pauli, T. M. Kutchan, *Plant J.* **13**, 793–801 (1998).
9. T. Morishige, T. Tsujita, Y. Yamada, F. Sato, *J. Biol. Chem.* **275**, 23398–23405 (2000).
10. A. Gesell *et al.*, *J. Biol. Chem.* **284**, 24432–24442 (2009).
11. R. Lenz, M. H. Zenk, *J. Biol. Chem.* **270**, 31091–31096 (1995).
12. T. Grothe, R. Lenz, T. M. Kutchan, *J. Biol. Chem.* **276**, 30717–30723 (2001).
13. J. M. Hagel, P. J. Facchini, *Nat. Chem. Biol.* **6**, 273–275 (2010).
14. B. Unterlinner, R. Lenz, T. M. Kutchan, *Plant J.* **18**, 465–475 (1999).
15. A. Nakagawa *et al.*, *Nat. Commun.* **2**, 326 (2011).
16. A. Nakagawa *et al.*, *Sci. Rep.* **4**, 6695 (2014).
17. K. M. Hawkins, C. D. Smolke, *Nat. Chem. Biol.* **4**, 564–573 (2008).
18. K. Thodey, S. Galanie, C. D. Smolke, *Nat. Chem. Biol.* **10**, 837–844 (2014).
19. W. De-Eknamkul, M. H. Zenk, *Phytochemistry* **31**, 813–821 (1992).
20. K. Hirata, C. Poeaknapo, J. Schmidt, M. H. Zenk, *Phytochemistry* **65**, 1039–1046 (2004).
21. R. S. Allen *et al.*, *Nat. Biotechnol.* **22**, 1559–1566 (2004).
22. T. Winzer *et al.*, *Science* **336**, 1704–1708 (2012).
23. Materials and methods are available as supplementary materials on *Science* Online.
24. F. P. Guengerich, A. W. Munro, *J. Biol. Chem.* **288**, 17065–17073 (2013).

25. F. Brodhun, C. Göbel, E. Hornung, I. Feussner, *J. Biol. Chem.* **284**, 11792–11805 (2009).
26. B. G. Hansen *et al.*, *Appl. Environ. Microbiol.* **78**, 4908–4913 (2012).
27. I. Hoffmann, F. Jernerén, E. H. Oliw, *J. Lipid Res.* **55**, 2113–2123 (2014).
28. The thousand plant transcriptomes project, www.onekp.com.
29. S. C. Farrow, P. J. Facchini, *J. Biol. Chem.* **288**, 28997–29012 (2013).

ACKNOWLEDGMENTS

We thank the laboratory and horticultural staff at GlaxoSmithKline Australia and the University of York for valuable technical assistance; J. Mitchell for administrative support; T. Davis for providing high–(*S*)-reticuline poppy straw; A. Bridges for providing DNA constructs; and D. Nelson for naming the P450 module. We acknowledge financial support from the UK Biotechnology and Biological Sciences Research Council (grant BB/K018809/1) and The Garfield Weston Foundation. The STORR cDNA sequence is available through the National Centre for Biotechnology Information under GenBank accession number KP998574. The University of York and GlaxoSmithKline have filed a patent application relating to this work. The supplementary materials contain additional data.

SUPPLEMENTARY MATERIALS

www.sciencemag.org/content/349/6245/309/suppl/DC1
Materials and Methods
Figs. S1 to S9
Tables S1 to S4
References (*30*–*42*)

25 March 2015; accepted 18 June 2015
Published online 25 June 2015;
10.1126/science.aab1852

CIRCADIAN RHYTHMS

Atomic-scale origins of slowness in the cyanobacterial circadian clock

Jun Abe,[1]* Takuya B. Hiyama,[1]* Atsushi Mukaiyama,[1,2]* Seyoung Son,[3]*† Toshifumi Mori,[2,4]* Shinji Saito,[1,2,4] Masato Osako,[3] Julie Wolanin,[1,5] Eiki Yamashita,[6] Takao Kondo,[3] Shuji Akiyama[1,2]‡

Circadian clocks generate slow and ordered cellular dynamics but consist of fast-moving bio-macromolecules; consequently, the origins of the overall slowness remain unclear. We identified the adenosine triphosphate (ATP) catalytic region [adenosine triphosphatase (ATPase)] in the amino-terminal half of the clock protein KaiC as the minimal pacemaker that controls the in vivo frequency of the cyanobacterial clock. Crystal structures of the ATPase revealed that the slowness of this ATPase arises from sequestration of a lytic water molecule in an unfavorable position and coupling of ATP hydrolysis to a peptide isomerization with high activation energy. The slow ATPase is coupled with another ATPase catalyzing autodephosphorylation in the carboxyl-terminal half of KaiC, yielding the circadian response frequency of intermolecular interactions with other clock-related proteins that influences the transcription and translation cycle.

Circadian clocks comprise suites of biological processes that oscillate with a 24-hour period (*1*). Clock genes and clock proteins are present in prokaryotes and eukaryotes (*2*, *3*); together, they constitute feedback loops that effect transcriptional and translational oscillations (TTOs). The origin of the slow circadian time scale is thought to be the time delay between clock gene transcription and feedback signals that regulate it; however, the transcriptional and translational events can occur quickly (i.e., within minutes) (*4*). Posttranslational oscillations (PTOs) (*5*–*7*) in biochemical modifications of clock proteins occur even without transcriptional and translational regulation. Proteins generally exhibit dynamics within picoseconds or seconds (*8*), much faster than the circadian time scale. Thus, both TTO and PTO circadian systems are assembled from building blocks with intrinsically fast dynamics, raising questions about how and why the systems are so slow and stable overall (*9*).

The cyanobacterium *Synechococcus elongatus* PCC7942 is the simplest organism known to have both TTOs (*10*) and PTOs (*5*). The *S. elongatus* PTOs can be reconstructed in vitro by incubating a core clock protein, KaiC, with two other clock proteins, KaiA and KaiB, and adenosine triphosphate (ATP) (*6*). The rhythmic behaviors of the Kai oscillator have been confirmed in many functional and structural analyses, which have probed the ATP hydrolysis [adenosine triphosphatase (ATPase)] activity of KaiC (*11*, *12*), autophosphorylation and autodephosphorylation activities of KaiC (*6*, *13*, *14*), conformational transitions of the proteins (*12*, *15*, *16*), and assembly or disassembly of Kai complexes (*17*–*20*). Because the PTO period in *S. elongatus* is firmly correlated to the TTO period during the day (*5*, *6*), the in vitro Kai oscillator should enable us to identify the mechanisms underlying the slowness of the circadian clock.

We searched the Kai oscillator for a minimal slow reaction whose efficiency correlated with in vivo TTO frequency (Fig. 1) (see supplementary materials and methods). The ATPase activity of full-length wild-type KaiC (KaiC-WT), consisting of the N-terminal C1 and C-terminal C2 domains, has been proposed as the basic timing cue (*11*, *12*). We identified the steady-state ATPase activity of the C1 domain (C1-ATPase) as a suitable slow reaction. A truncated version of KaiC consisting solely of the N-terminal domain, KaiC1-WT, exhibited much slower ATP hydrolysis (11 ± 1 ATP per day per KaiC at 30°C) than well-known motor proteins (10^3 to 10^7 day^{-1}) such as myosin, kinesin, and F_1-ATPase (table S1). We confirmed the correlation of this activity with the in vivo TTO frequency using a series of period-modulating KaiC mutations in the C1 domain [$S^{157}\rightarrow P^{157}$ (S157P), S157C, T42S, S48T] (*21*) (Fig. 1D), in which higher steady-state C1-ATPase in vitro resulted in higher-frequency TTOs in vivo. Thus, KaiC should experience a certain number of hydrolysis events per cycle in vivo, and the absolute rate of ATPase activity is connected to the cellular clock's overall slowness (*11*, *22*). Therefore, we examined the structural origin of the slow C1-ATPase and its coupling with TTOs via spatiotemporally distinct events, including the intramolecular KaiC ATPase and its phosphorylation cycles, as well as intermolecular interactions with KaiA and KaiB (Fig. 1).

To this end, we crystallized KaiC1-WT and five period-modulating variants in the pre- or posthydrolysis states, or both. All resultant crystals were in the $P2_12_12_1$ space group (Fig. 2, A and B, fig. S1, and table S2). The prehydrolysis states (Fig. 2A, blue subunits) exhibited common features: assembly of six subunits into a hexamer and incorporation of one molecule of the slowly hydrolyzed ATP analog adenosine 5′-(γ-thiotriphosphate) (ATP-γ-S) into every subunit-subunit interface. ATP-γ-S existed in a complex with a Mg^{2+} ion (Mg-ATP-γ-S) in the ordinary octahedral-coordination geometry (fig. S2A). We observed the posthydrolysis state of the long-period variant KaiC1-S48T (Fig. 2B, orange and green subunits), which crystallized as an asymmetrically ATP- or adenosine diphosphate (ADP)–bound hexamer (fig. S2B). The ring-shaped hexamer was deformed asymmetrically due to steric constraints resulting from close juxtaposition of three types of subunits, creating both tight and loose intersubunit interfaces (Fig. 2B, fig. S3, and supplementary text).

We identified two structural sources of slow ATPase activity. The first is the regulatory influence of the protein moiety on a lytic water molecule (W1) near the phosphorus atom (P_γ) of the γ-phosphate group of an ATP. In the prehydrolysis state (blue dotted box in Fig. 2C), W1 was sequestered (with a W1–P_γ distance of 3.8 to 3.9 Å and a W1–P_γ–$O_{3\beta}$ angle of 154° to 158°) by

[1]Research Center of Integrative Molecular Systems (CIMoS), Institute for Molecular Science, 38 Nishigo-Naka, Myodaiji, Okazaki 444-8585, Japan. [2]Department of Functional Molecular Science, SOKENDAI (The Graduate University for Advanced Studies), 38 Nishigo-Naka, Myodaiji, Okazaki 444-8585, Japan. [3]Division of Biological Science, Graduate School of Science, Nagoya University, Furo-cho, Chikusa-ku, Nagoya 464-8602, Japan. [4]Department of Theoretical and Computational Molecular Science, Institute for Molecular Science, 38 Nishigo-Naka, Myodaiji, Okazaki 444-8585, Japan. [5]PSL Research University, Chimie ParisTech, 75005 Paris, France. [6]Institute for Protein Research, Osaka University, 3-2 Yamada-oka, Suita 565-0871, Japan.
*These authors contributed equally to this work. †Present address: College of Pharmacy, Chungbuk National University, 410 Seongbong-ro, Heungdeok-gu, Cheongju, Chungbuk 361-763, Korea. ‡**Corresponding author. E-mail: akiyamas@ims.ac.jp**

www.sciencemag.org/cgi/content/full/science.aab1852/DC1

Supplementary Materials for

Morphinan biosynthesis in opium poppy requires a P450-oxidoreductase fusion protein

Thilo Winzer, Marcelo Kern, Andrew J. King, Tony R. Larson, Roxana Teodor, Samantha Donninger, Yi Li, Adam A. Dowle, Jared Cartwright, Rachel Bates, David Ashford, Jerry Thomas, Carol Walker, Tim A. Bowser, Ian A. Graham*

*Corresponding author. E-mail: ian.graham@york.ac.uk

Published 25 June 2015 on *Science* Express
DOI: 10.1126/science.aab1852

This PDF file includes:

Materials and Methods

Generation of EST libraries by pyrosequencing and contiguous assembly

Generation of EST libraries by pyrosequencing and contiguous assembly of the HM2 cultivar was performed as described previously (*28*).

Generation and field-based screening of an ethyl methanesulfonate (EMS) mutagenized mutant population

Seeds of the *P. somniferum* high morphine cultivar HM2 were mutagenized with EMS. Prior to mutagenesis, M1 seeds were soaked in 0.1% (w/v) potassium chloride solution for approximately 24 hours. The seed was then imbibed for three hours with ethyl methanesulfonate solution (200 mM EMS in 100 mM sodium hydrogen phosphate buffer, pH 5.0, supplemented with 700 mM dimethyl sulfoxide). The treated M1seed was washed twice for 15 min each with 100 mM sodium thiosulphate solution and then twice for 15 min each with distilled water. A volume of 10 mL of the respective solutions was used per 1000 seeds and all steps were carried out on a rocking platform. The washed M1 seed was dried overnight on Whatman 3MM Blotting paper (Whatman/GE Healthcare Life Sciences, Little Chalfont, UK) and sown the following morning on top of a mixture of John Innes no 2 compost, vermiculite and perlite (4:2:1), then covered with a thin layer of compost. Seedlings were transplanted three to four weeks after germination into larger pots and grown in the glasshouse until maturity. Dried capsules were harvested by hand from the M1 population once capsules had dried to approximately 10% moisture on the plant. M2 seed was manually separated from the capsule and used to generate the M2 seed families used in the field-based trials described below.

M2 seed lines from the EMS mutagenised population were grown in 2 m long rows in the field in Tasmania in the 2009/2010 growing season. Plants were thinned to 75 mm apart, grown, and 4 plants per M2 line were self-pollinated. Poppy capsules were harvested from the respective mutant lines once capsules had dried to approximately 10% moisture on the plant. Extraction and alkaloid analyses of field-grown material were carried out as described previously (*28*).

Analysis of selected self-pollinated capsules from some M2 plant lines indicated significantly reduced morphinan amounts, and significantly higher amounts of reticuline. M3 seeds from these capsules were sown in the following growing season in Tasmania to confirm the phenotype.

Generation of segregating F2 populations

Segregating F2 populations were set up for the three mutant lines identified in the field-based screen. Plants homozygous for *storr-1*, *storr-2* and *storr-3*, respectively, were crossed to recurrent morphinan containing parents. The resulting F1 generation was self-pollinated to produce segregating F2 populations.

Isolation and sequencing of the full-length STORR cDNA from wild type HM2 and three high reticuline mutant lines

Papaver somniferum plants of the wild type HM2 cultivar as well as three high reticuline EMS mutant lines were grown under glasshouse conditions to post-flowering stages (1-6 days after petal fall) and stem segments (2.5-3 cm long) immediately beneath

the flowers were harvested and flash frozen in liquid nitrogen. Total RNA was extracted from the stems using the pine tree RNA extraction method (*30*) and further purified using the RNeasy Plus MicroKit (Qiagen, Crawley, UK). RNA quality and purity were checked using the RNA ScreenTape system and analysed with the 2200 TapeStation Software (Agilent Technologies, Wokingham, UK).

Total RNA samples (1 µg) from high reticuline mutants and wild-type lines were treated with RQ1 DNAse (Promega, Southampton, UK) following the manufacturer's instructions. cDNA synthesis was performed using 10 µM oligo dT MW 4500 (Invitrogen/Life technologies, Paisley, UK) and 1 mM dNTP. Reactions were incubated for 5 min at 65°C to allow annealing of oligonucleotides. First strand synthesis reactions contained 1 × First Strand buffer (Invitrogen/Life Technologies), 20 mM DTT, 40 U RNAse out (Invitrogen/Life technologies). Reactions were incubated at 42°C for 2 min and then 200 U SuperScript II reverse transcriptase (Invitrogen/Life technologies, Paisley, UK) was added followed by a 50 min incubation at 42°C and heat inactivation at 70°C for 15 min. Samples were diluted 5 × in water and used for gene specific amplifications.

The full-length region encoding the CYP82Y2-oxidoreductase gene was amplified from the cDNA samples using the primers 5'-GGGTTGAATCATGGAGCTC-3', 5'-GAAGGGAATGAGATCCGTGAC-3' and the high fidelity Q5® Hot Start High-Fidelity DNA Polymerase (New England Biolabs, Hitchin, UK) according to the guidelines supplied by the manufacturer. Cycling conditions were as follows: 98°C for 30 s, 35 cycles of 98°C for 10 s, 64°C for 30 s, 72°C for 2.5 min and a final extension at 72°C for 3 min. The 3 kb-PCR product was then ligated into the pSC-A vector using the Strataclone PCR Cloning Kit (Agilent Technologies) and the individual clones were fully sequenced so that at least 3 clones were obtained from each one of the wild-type and mutant poppy lines.

Genotyping and alkaloid profiling of segregating F2 populations

Leaf samples (30-50 mg) for DNA extraction were harvested from 4-6 week old plants growing in the glasshouse. Genomic DNA was extracted using the BioSprint 96 Plant kit on the BioSprint 96 Workstation (Qiagen, Crawley, UK) according to the manufacturer's protocol. Extracted DNA was quantified on the NanoDrop™ 8000 Spectrophotometer (Fisher Scientific, Wilmington, DE, USA) and normalized to 10 ng/µL. KASP genotyping assays were used to genotype the F2 populations described above. To design allele-specific primers, sequences of 50-100 nucleotides around the mutation site were submitted to LGC genomics (Hoddesdon, UK) to order KASP by Design (KBD) primer mix.

Reactions were carried out in FrameStar® 384 well plates (4titude® Ltd, Wotton, UK) in a total volume of 5.22 µL volume per reaction, with reaction components in the following final concentrations: 1 × KASP V4.0 mastermix (LGC genomics); 1 × KBD primer mix; 3% HiDi Formamide (Life Technologies, Paisley, UK); 10 ng DNA, HyClone molecular grade water (Thermo Scientific, Hemel Hempstead, UK) to total volume. The plates were centrifuged for 2 min at 4500 × g, heat-sealed using the Kube™ heat-based plate sealer (LGC genomics), and thermal cycling was carried out in a Hydrocycler™ (LGC genomics) water bath-based thermal cycler, with the following conditions: 94°C for 15 min; 10 cycles: 94°C for 20 s, 61-55°C for 60 s (dropping 0.6°C

per cycle); 38 cycles: 94°C for 20 s, 55°C for 60 s. The plate reading was carried out on an Applied Biosystems ViiA7 instrument (Life Technologies) using short reads of 30 s at 25°C.

The sequences of the allele-specific primers as well as the common primer used in the KASP genotyping assays were as follows:

Mutant allele	Primer	Primer sequence (5' to 3')	Label
storr-1	wild type allele	ATCAGCGTGAGCATCAGTGCAC	Hex
	mutant allele	GATCAGCGTGAGCATCAGTGCAT	FAM
	common primer	TCTCGAGATGAACTTTTCATCAGTTCCAT	
storr-2	wild type allele	CGTAAGACCTGTCAATTGGTCAATC	FAM
	mutant allele	CGTAAGACCTGTCAATTGGTCAATT	HEX
	common primer	TCCAGTGTCAGATAATGTTCCAATGCTA	
storr-3	wild type allele	GTGGACATGACAGCAACACCAG	FAM
	mutant allele	AAAGTGGACATGACAGCAACACCAA	HEX
	common primer	CAAGGGGGATCACCTTGTAACTCAT	

Capsule straw analysis of a glasshouse grown F2 population segregating *storr-1* was performed as described previously (*28*). Leaf latex analysis of glasshouse grown F2 populations segregating *storr-2* and *storr-3*, respectively, was carried out as follows: Latex was collected when the first flower buds emerged (~7 week old plants) from cut petioles, with a single drop dispersed into 500 µL of 10% acetic acid. This was diluted 10 × in 1% acetic acid to give an alkaloid solution in 2% acetic acid for further analysis. Alkaloids were analysed as described previously for the capsule straw analysis of glasshouse grown material (*28*). The relative content of alkaloids was measured as % peak area relative to total alkaloid peak area.

Complementation tests

Crosses were carried out between *storr-1* × *storr-2*, *storr-1* × *storr-3* and *storr-2* × *storr-3*. Ten day old seedlings of the respective F1s as well as the parental lines and HM2 were extracted in 10 % acetic acid (5µL 10 % acetic acid per mg fresh weight) with a mortar and pestle. The homogenate was centrifuged twice at 12,000 × g and 4°C. The cleared supernatant was analysed on LCMS using the TFA method as described below. 10 seedlings were used for each of three biological replicates.

Cloning and expression and ^{15}N-labeling of recombinant STORR protein for use in mass spectrometry applications

A sequence verified wild type *STORR* cDNA clone was used as template in a PCR-based sub-cloning reaction to provide a protein expression construct with an N-terminal 6HIS tag. Briefly, the mature coding region was amplified from the template plasmid using the polymerase chain reaction and the oligonucleotide forward and reverse primers; d(TCCAGGGACCAGCAATGGAGCTCCAATATATTTCTTATTTTCAAC) and d(TGAGGAGAAGGCGCGTTAAGCTTCATCATCCCACAACTCTTC) , respectively. After amplification with KOD Hot-Start DNA polymerase (Novagen), the DNA product was recovered by purification (Qiagen) and combined with the destination vector pETLIC3C (*31*) using an InFusion cloning reaction (prepared according to the

manufacturers recommendations). The resulting construct yielded an N-terminal fusion of a 6HIS tag with a 3C-protease cleavage site (pETLIC3C) under the control of the T7 promoter. The plasmids were transformed in *E. coli* XL1-Blue (Stratagene) cells for propagation and the cloning was confirmed by DNA sequence analysis.

Routine protein expression was performed in *E. coli* strain BL21(DE3) (Novagen) by inoculating a single colony from an LB agar plate containing 30 μg/ml kanamycin into 10 ml of LB medium containing 30 μg/ml kanamycin. After 16 hours incubation at 37°C and 200 rpm, the starter-culture was transferred to 500 ml LB medium containing 30 μg/ml kanamycin and incubated at 37°C, 180 rpm until an OD600 nm of 0.6 AU was obtained. Induction was then achieved by the addition of IPTG to a final concentration of 1mM before incubation was continued for 4 hours. The induced cells were harvested by centrifugation at 5,000 × g, washed (phosphate buffered saline), and the pellet stored at -80°C until required for protein purification. Protein expression of recombinant ^{15}N-labeled STORR was performed in *E. coli* strain ArcticExpress(DE3) (Agilent Technologies) by inoculating a single colony from an LB agar plate containing 1% (w/v) glucose, 30 μg/ml kanamycin into 10 ml of LB medium containing 1% (w/v) glucose, 30 μg/ml kanamycin. After 16 hours incubation at 37°C and 200 rpm, the starter-culture was centrifuged at 2,700 × g for 5 min at 20°C and the cell pellet resuspended in 750 ml ^{15}N-labeled M9 minimal media (^{15}N ammonium chloride, Cambridge Isotope Laboratories, Inc., Tewksbury, MA, USA) containing 30 μg/ml kanamycin and incubated at 37°C, 180 rpm until an OD600 nm 0.6Au was obtained. Induction was then achieved by the addition of IPTG to a final concentration of 1mM before incubation was continued for 4 hours. The induced cells were harvested by centrifugation at 5,000 × g, washed (phosphate buffered saline), and the pellet stored at -80°C until required for protein purification.

The purification of routine and ^{15}N-labeled protein was performed using the following procedure. Frozen cell pellets were thawed and resuspended in lysis buffer (20 mM Tris-HCl, pH 8.0, 150 mM NaCl, 1mM DTT containing protease inhibitor cocktail (Roche)) prior to disruption using sonication. A pellet was then recovered by centrifugation at 12,000 × g for 10 min at 4°C and washed twice by resuspending in lysis buffer and centrifuging as above. The washed pellet was then incubated in solubilisation buffer (25 mM Tris-HCl, pH 8.0, 8 M guanidine HCL and 1mM DTT) by gently mixing at 4°C for 16h before the solution was clarified by filtration through a 0.8 μm syringe filter (Sartorius, Epsom, UK). The filtrate was then further purified by loading the extract at a flow rate of 1ml/min onto Ni^{2+}-affinity chromatography using a HiTrap column (GE Healthcare) previously equilibrated in Buffer A (50 mM sodium phosphate, pH 8.0, 300 mM NaCl, 6 M urea and 20mM imidazole). On completion of sample loading, the column was washed with 10 column volumes (CV) of Buffer A before step elution of specific protein using 5 CV Buffer B (50mM sodium phosphate, pH 8.0, 300 mM NaCl, 6 M urea and 500mM imidazole). Fractions containing the STORR expressed protein were confirmed by SDS-PAGE and the protein concentration estimated by A_{280} nm. Analysis of the purified recombinant STORR protein showed full-length expression at the anticipated molecular weight of 103 kDa. The identity of this protein as STORR was confirmed by tryptic digestion and peptide mapping. Likewise, a second product at approximately 40 kDa was confirmed to be an N-terminal fragment of the CYP82Y2 module of the STORR protein. For the relative quantification of the native STORR

protein in opium poppy stem extracts only the full length ^{15}N-labeled recombinant STORR protein was used.

Preparation of crude protein extracts from stems of wild type high morphine cultivar HM2

Stem tissue from just below the flower was harvested from HM2 wild type plants shortly after onset of anthesis. The tissue samples were immediately frozen in liquid nitrogen and stored at -80°C until extraction. For each biological replicate, stem samples from 3-5 plants were ground together in liquid nitrogen to a fine powder with a mortar and pestle. 200 mg of tissue powder was extracted with 300 µL of 1.5 × cracking buffer (preparation of 5× cracking buffer: 1 mL 0.5 M Tris-HCl, pH 6.8, 1.6 mL glycerol, 1.6 mL 10% (w/v) SDS, 0.4 mL 2-mercaptoethanol, 0.4 mL 5% (w/v) bromophenol blue, 3 mL H_2O). The samples were vortexed thoroughly until a homogeneous suspension was achieved. The suspension was incubated for 5 min at 95°C, vortexed for 1 min and then centrifuged at 16,000 × g in a bench top centrifuge. 200 µL of the cleared supernatant was transferred into a fresh tube and used for SDS-PAGE.

SDS-PAGE separation of wild type HM2 stem crude protein extracts and recombinant

A 40 µL aliquot of each biological replicate was run on a 7 cm NuPAGE Novex 4-12% Bis-Tris gel (Life Technologies) at 200 V until the 25 kDa mass marker (PageRuler Plus, prestained protein ladder - Thermo Scientific, Huntingdon, UK) reached the bottom of the gel. The gel was stained with SafeBLUE protein stain (NBS biologicals) for 1 hour before destaining with ultrapure water for 1 h.

In-gel tryptic digestion

Each gel lane was divided into 15 regions (Fig. 2) before excision to LoBind tubes (Eppendorf, Stevenage, UK), washed twice with 50% (v:v) aqueous acetonitrile containing 25 mM ammonium bicarbonate, reduced with DTT (10 mM) and alkylated with iodoacetamide (50 mM). Following dehydration with acetonitrile, gel pieces were digested with 0.2 µg sequencing-grade, modified porcine trypsin (Promega) at 37°C overnight. Peptides were extracted from the gel by washing three times with 50% (v:v) aqueous acetonitrile, before drying in a vacuum concentrator and reconstituting in 0.1% (v:v) aqueous trifluoroacetic acid.

LC-MS/MS peptide analysis

The tryptic digests were loaded onto a nanoAcquity UPLC system (Waters, Elstree, UK) equipped with a nanoAcquity Symmetry C_{18}, 5 µm trap (180 µm × 20 mm Waters) and a nanoAcquity HSS T3 1.8 µm C_{18} capillary column (75 µm × 250 mm, Waters). The trap wash solvent was 0.1% (v/v) aqueous formic acid and the trapping flow rate was 10 µL/min. The trap was washed for 5 min before switching flow to the capillary column. The separation used a gradient elution of two solvents (solvent A: 0.1% (v/v) formic acid; solvent B: acetonitrile containing 0.1% (v/v) formic acid). The flow rate for the capillary column was 300 nL/min. Column temperature was 60°C and the gradient profile was linear 2-30% B over 125 min then linear 30-50% B over 5 min. The column was washed with 95% solvent B for 2.5 min, returned to initial conditions and re-equilibrated for 25 min before subsequent injections.

The nanoLC system was interfaced to a maXis HD LC-MS/MS System (Bruker Daltonics, Coventry, UK) with a CaptiveSpray ionisation source (Bruker Daltonics). Positive ESI- MS & MS/MS spectra were acquired using AutoMSMS mode. Instrument control, data acquisition and processing were performed using Compass 1.7 software (microTOF control, Hystar and DataAnalysis, Bruker Daltonics). Instrument settings were: ion spray voltage: 1,450 V, dry gas: 3 L/min, dry gas temperature 150 °C, ion acquisition range: *m/z* 150-2,000, quadrupole low mass: 300 *m/*z, transfer time: 120 ms, collision RF: 1,400 Vpp, MS spectra rate: 5 Hz, cycle time: 1 s, and MS/MS spectra rate: 5 Hz at 2,500 cts to 20 Hz at 250,000 Hz. The collision energy and isolation width settings were calculated automatically using the AutoMSMS fragmentation table, absolute threshold 200 counts, preferred charge states: 2 – 4, singly charged ions excluded. A single MS/MS spectrum was acquired for each precursor and former target ions were excluded for 0.8 min unless the precursor intensity increased fourfold.

Relative quantification of STORR protein in SDS-PAGE fractions

Recombinant, ^{15}N-labeled (heavy) STORR protein was used as an internal standard. An equal amount of a tryptic digest of heavy protein was spiked into the in-gel digest of each SDS-PAGE region, and the spiked regions were analysed by LC-MS/MS as described above. Extracted-ion chromatograms (EIC) were created using DataAnalysis version 4.2 (Bruker Daltonics) for multiply-protonated molecule species of the heavy and light (endogenous) versions of the following STORR peptides:

			Calculated *m/z*	
Peptide sequence	**Predicted sequence position**	***z***	**Light**	**Heavy**
YGPIFSFPTGSHR	90-102	3	489.246	495.228
IVCGFQSGPK	234-243	2	546.779	552.761
LYPASPVVER	433-442	2	565.814	572.295
IKPCVQSAASER	568-579	3	449.235	454.885
IGEIPQCR	869-876	2	486.750	492.732

The EIC mass tolerance was 10 mDa and the chromatograms were baseline subtracted and smoothed before integration with the following parameters: signal/noise threshold, 3; intensity threshold, 3%. The ratio of light to heavy peptides (L:H) was calculated from the resulting integrated EIC peak areas.

Reticuline standards and isolation of (*S*)-reticuline for enzymatic assays

Authentic standards of (*R*)-reticuline (Santa Cruz Biotechnology, Dallas, TX) and (*S*)-reticuline (Toronto Research Chemicals, Toronto, ON) were prepared as 10 mM stock solutions in methanol + 0.1 % acetic acid. 1,2-dehydroreticuline was obtained from US Biologicals (Salem, MA, USA) or Toronto Research Chemicals (Toronto, Canada) and prepared as a 10 mM stock solution in DMSO. (*S*)-reticuline for use in assays was prepared from a mutant poppy line known to contain a high content of (*S*)-reticuline, and verified as >99.8% pure by chiral analysis compared to the authentic standards.

The poppy capsule was deseeded to produce poppy straw which was then ground to a fine powder using a Retsch (Haan, Germany) SM300 cutting mill at 2600 rpm with a ≤ 1 mm screen. The milled straw was then extracted using a four stage solid-liquid counter-current method. Four batches of 50 g poppy straw and 3.5 g calcium oxide were prepared. To the first batch, 500 mL of water was added and the resulting slurry was stirred at room temperature for 25 - 35 min. The slurry was filtered and 200 mL of the aqueous extract was removed and added to the second batch of straw and the volume brought up to 500 mL with water. The process was repeated such that each batch of straw had been extracted four times. The four 200 mL extracts were then combined to make 800 mL of aqueous alkaloid rich extract at pH 12.3. Sodium carbonate (25 g) was then added to precipitate calcium carbonate. After 15 min of stirring, the extract was filtered through Celite filter aid. The pH was then adjusted to 3-4 using 10% v/v sulphuric acid and the solution filtered through Celite. The extract was adjusted to pH 9.2 with 10% v/v sodium hydroxide and extracted three times with 200 mL of dichloromethane and the solvent was removed by rotary evaporation. The extract was then dissolved in 2% methanol, 1 % acetic acid and purified by reverse phase (C18) silica gel flash chromatography using a 2% to 50 % methanol in 1 % acetic acid gradient. The (*S*)-reticuline containing fractions were then dried in a speedvac at room temperature, and used to prepare stock solutions at 10 mM in methanol + 0.1 % acetic acid.

Heterologous protein expression in yeast

Genscript created synthetic DNA sequences were created for PsCPR [Genbank accession AAC05021, (*32*)], the full length STORR (CYP82Y2-Oxired) protein, the N-terminal CYP82Y2 module and C-terminal oxidoreductase (Oxired) module , that were codon optimised for expression is *Saccharomyces cerevisiae*. The codon-optimized sequences are provided in figures S6-9.

The codon optimized genes were then amplified by PCR using the following primers which incorporate a restrictions site and 5'-AAAA-3' Kozak sequences preceding the start codon:

Primer name	**Target**	**Sequence**
CPR_XhoI_F CPR_BamHI_R	Codon optimized cytochrome P450 reductase (CPR)	5'-AAAAGGATCCAAAAATGGGTTCAAACAACTTAGCCAACTC-3' 5'-AAAACTCGAGTTACCAAACATCTCTCAAATATCTTTCTTC-3'
CYP82Y2-oxired_NotI_F CYP82Y2-oxired_PacI_R	Codon optimized full-length CYP82Y2-oxired fusion protein	5'-AAAAGCGGCCGCAAAAATGGAATTACAATACATCTCCTACTTTC-3' 5'-AAAATTAATTAATTATGCTTCGTCATCCCATAATTC-3'
CYP82Y2_NotI_F CYP82Y2_PacI_R	Codon optimized N-terminal CYP82Y2 module	5'-AAAAGCGGCCGCAAAAATGGAATTACAATACATTTCTTACTTTC-3' 5'-AAAATTAATTAATCTCTTTCAGATGCAGCAC-3'
oxired_NotI_F oxired_PacI_R	Codon optimized C-terminal oxired module	5'-AAAAGCGGCCGCAAAAATGGAATCCTCTGGTGTCCCTG-3' 5'-AAAATTAATTAATTATGCTTCGTCATCCCACAATTC-3'

Expression vector pESC-TRP::soloxired was created by digesting the corresponding PCR product with NotI and PacI and inserting this behind the *GAL10* promoter of pESC-TRP. pESC-TRP::CPR was created by digesting the corresponding PCR product with BamHI and XhoI and inserting this behind the *GAL1* promoter of pESC-TRP. This was then used to created pESC-TRP::CPR::CYP82Y2 and pESC-TRP::CPR::CYP82Y2-oxired. These plasmids were then transformed in *S. cerevisiae* G175 (*33*) using lithium acetate protocol (*34*). Yeasts were cultivated in Synthetic Defined (SD) medium composed of 2 % carbon source, 0.5 % ammonium sulfate, 1.7 g L^{-1} yeast nitrogen base (without amino acids and ammonium sulfate) and 1.92 g L^{-1} or tryptophan drop-out supplement (Sigma-Aldrich, Gillingham, UK). Cultures grown using glucose as a carbon source were used to inoculate 200 ml cultures with raffinose as a carbon source to an OD 600 nm of 0.10 in 1 L conical flasks. These were grown at 30 ºC, 250 rpm, and at and OD 600 nm of 1.8 to 2.2, 20 mL of 20 % galactose was added to induce expression on the plasmid-borne transgenes. After a further 16 hours of cultivation, the yeast cells were harvested by centrifugation at 2,000 *g* for 10 min. The yeast cells were then washed once with 50 mL of water, then suspended in 2 mL of extraction buffer containing 100 mM Bis-tris propane (pH 8.0), 1.2 M sorbitol, 100 mM NaCl, 1 mM EDTA, 1 mM DTT and 1/250 dilution of protease inhibitor cocktail (Sigma-Aldrich P8215). Soluble and microsomal preparations were then prepared as described previously (*35*).

Creation of *STORR* mutant variants for heterologous expression in yeast.

STORR variants were also created from codon-optimized templates and introduced into the pESC-TRP::CPR vector to create pESC-TRP::CPR::STORR1, pESC-TRP::CPR::STORR2 and pESC-TRP::CPR::STORR3. The *STORR1* variant was created by PCR using the CYP82Y2-oxired_NotI_F primer (above) and 5'-AAAATTAATTAATCACAACATAGAACTTATAAACAATTCATCTC-3'.The *STORR2* variant was created using the CYP82Y2_NotI_F primer and 5'AAAATTAATTAATCAACCCAACATAGGGACATTATCAG-3'. The *STORR3* variant was created using overlap extension PCR (*36*). The 5' fragment was created using primer CYP82Y2-oxired_NotI_F and 5'-CTTTGTAAGACATCAATCTTGGTGTAGCAGTCATATC-3' and the 3' fragment using primer 5'- GATATGACTGCTACACCAAGATTGATGTCTTACAAAG-3' and CYP82Y2-oxired_PacI_R.

Enzyme assays

Enzymes assays were set up with final concentrations of 50 mM Bis-tris propane buffer (pH 8), 50 mM NaCl, 1 mM NADPH, 100 µM of substrate and crude soluble protein preparation (1 mg mL^{-1} protein) or crude microsomal protein preparation (6 mg mL^{-1} protein). The assays were incubated at 37 ºC for 3 hours. For non-chiral analysis, the assays were terminated by the addition of an equal volume of methanol + 1 % acetic acid containing 100 µM noscapine as an internal standard. The reaction was then centrifuged at 20,000 *g* for 2 minutes, and the supernatant recovered for analysis of DHR and (*R/*S)-

reticuline content (i.e., non-chiral method). For chiral analysis of reticuline, the reaction was terminated by the addition of an equal volume of 0.5 M sodium carbonate buffer (pH 10.0). Reticuline was then extracted from the reaction products by three sequential extractions with two volumes of dichloromethane. The solvent extracts were combined and evaporated to dryness in a speedvac. The extract was then dissolved in 50:50:0.1 hexane/ethanol/diethylamine and analysed by the chiral LC-MS method to determine the relative amounts of (*R*)- and (*S*)-reticuline.

For kinetic experiments, reactions were performed in 100 µL volumes containing 50 mM Bis-tris propane buffer, 50 mM NaCl, 2 mM NADPH, 6 mg mL^{-1} microsomal protein and 1-500 µM of substrate. 10 µL aliquots were withdrawn at different time intervals and quenched with 40 µL of 25% methanol, 1% acetic acid containing 2.4 µM noscapine.

Analysis of benzylisoquinoline alkaloids by LCMS

Poppy capsules were processed and analysed by UPLC-MS and R-scripts as previously described ("the standard method"; (*28*)). Compounds were annotated by generation of empirical formulae from exact masses (< 5 ppm mass accuracy) and comparison to authentic standards. High resolution MS-based identifications and quantifications were performed after matching theoretical to found $[M+H]^+$ pseudomolecular ions within a 10 ppm error window. In all experiments where quantifications are reported for 1,2- dehydroreticuline (calculated m/z = 328.1543) or reticuline (calculated m/z = 330.1700), mass errors did not exceed 5 ppm. Unknowns were annotated by a masstag in the format MxTy, where x is mass and y is retention time in seconds. The standard method did not resolve reticuline epimers, so chiral separation methods were developed specifically for this purpose. These were based on methods described by Iwasa *et al.* (*37*), and achieved using Lux cellulose 3 columns (Phenomenex, Macclesfield, UK) with isocratic separations employing hexane:ethanol:diethylamine (50:50:0.1 v/v) as mobile phase. Extracted samples were dried and reconstituted in this solvent prior to analysis. Two separation systems were used; the first used a 250 × 4.6 mm column with a 5 µm particle size on a TSP HPLC system interfaced to LCQ mass spectrometer operating in positive APCI mode (Thermo Separation Products, Hemel Hempstead, UK). On this system, the injection volume was set to 10 µL, the column temperature to 40 °C and the flow rate to 0.5 mL/min. Under these conditions, (*S*)- and (*R*)-reticuline eluted at 10.8 and 14.0 min, respectively. This system was used to analyse reticuline epimers from capsule extracts. A second system with increased sensitivity was used to analyse epimers from *in vitro* assays. This used a 100 × 4.6 mm column with a 3 µm particle size on the Waters Acquity UPLC system interfaced to an LTQ-Orbitrap mass spectrometer operating in positive APCI mode described previously (*28*). The same separation conditions were used as described for the LCQ system, but with the injection volume reduced to 2 µL. Under these conditions, (*S*)- and (*R*)-reticuline eluted at 4.3 and 5.5 min, respectively. 1,2-dehydroreticuline from capsules could not be measured with the chiral methods, but was successfully measured using the standard method. However aliquots from *in vitro* assays exhibited irreproducible retention times and poor peak shapes for this compound. Measurement of this analyte from *in vitro* assays was achieved under ion-pairing conditions.

TFA-method: For selected 1,2-dehydroreticuline analyses, the UPLC-MS system was fitted with a Luna HST C18(2) column (Phenomenex) with dimensions 50 x 2 mm and a 2.5 µm particle size. Solvent A was water and solvent B was methanol, both with 0.1% (v/v) trifluoroacetic acid (TFA) added. Samples were injected in 2 µL and eluted at 37 °C and 0.5 mL/min on the column over the following linear gradient: initial 2 min isocratic 98% A; 2 – 8 min to 98% B. Under these conditions, 1,2-dehydroreticuline eluted at 4.0 min.

Phylogenetic analysis of the STORR cytochrome P450 and oxidoreductase modules

The N-terminal cytochrome P450 module was used as query sequence in a BLASTP search in the curated Swissprot database via on the NCBI webpage (http://www.ncbi.nlm.nih.gov/). The top hits (expected value less than 1E-70) were retrieved, which included all members from the plant specific CYP82 subfamily and some members from the CYP71, CYP75 and CYP93 subfamilies. Other sequences were also included: CYP82E4v1_TOBAC (ABA07805.1), CYP82E4_NICTO (ABM46920.1), CYP82E4v2_TOBAC (ABA07804.1), CYP82E3_NICTO (ABM46919.1), AII31758_GOSHI (AII31758.1), AII31760_GOSHI (AII31760.1), AII31759_GOSHI (AII31759.1), CYP82G1_ARALY (EFH61953.1), CYP82F1_ARALY (EFH56916.1), AAS90126_AMMMJ (AAS90126.1), NMCH_ESCCA (AAC39454.1), CYP82X1_PAPSO (AFB74614.1), CYP82X2_PAPSO (AFB74616.1), CYP82Y1 (AFB74617.1). Sequences were retrieved from SwissProt or GenBank databases (http://www.ncbi.nlm.nih.gov/). After initial alignment with ClustalX and phylogenetic analysis, only members of the CYP82 subfamily were included in the final analysis.

The C-terminal oxidoreductase module was used as query sequence in a PSI-BLAST search (*40*) in the Swissprot database on the NCBI website, the search converged after 9 iterations with threshold set at 1E-10. The search result included 250 hits from plants, animals, fungi, protists and bacteria. All plant sequences were retrieved and further aldo/keto-reductase 4 sequences were added (*41*). After the initial alignment and phylogenetic analysis, only members of the plant specific aldo/keto-reductase 4 subfamily were included in the final analysis.

Species-specific identifiers have been assigned identifier as follows: *Ammi majus* (_AMMMJ), *Arabidopsis lyrata* (_ARALY), *Arabidopsis thaliana* (_ARATH), *Digitalis purpurea* (_DIGPU), *Erythroxylum coca* (_ERYCB), *Eschscholzia californica* (_ESCCA), *Fragaria x ananassa* (_FRAAN), *Glycyrrhiza glabra* (_GLYGL), *Gossypium hirsutum* (_GOSHI), *Glycine max* (_SOYBN), *Hordeum vulgare* (_HORVU), *Malus domestica* (_MALDO), *Medicago sativa* (_MEDSA), *Nicotiana tabacum* (_TOBAC), *Nicotiana tomentosiformis* (_NICTO), *Oryza sativa* Japonica (_ORYSJ), *Panax ginseng* (_PANGI), *Papaver somniferum* (_PAPSO), *Pisum sativum* (_PEA), and *Sesbania rostrata* (_SESRO).

GenBank accession numbers for the protein sequences are as follows:

Cytochrome P450s: CYP82A3_SOYBN (O49858.1), CYP82A1_PEA (Q43068.2), CYP82A4_SOYBN (O49859.1), CYP82A2_SOYBN (O81972.1), CYP82D1_GOSHI (AII31758.1), CYP82D2_GOSHI (AII31759.1), CYP82D3_GOSHI (AII31760.1), CYP82D47_PANGI (H2DH24.1), CYP82E4v1_TOBAC (ABA07805.1), CYP82E4_NICTO (ABM46920.1), CYP82E4v2_TOBAC (ABA07804.1), CYP82E3_NICTO (ABM46919.1), CYP82G1_ARALY (EFH61953.1),

CYP82G1_ARATH (Q9LSF8.1), NMCH_ESCCA (AAC39454.1), CYP82C4_ARATH (Q9SZ46.1), CYP82C3_ARATH (O49396.3), CYP82C2_ARATH (O49394.2), AAS90126_ CYP82H1 AMMMJ (AAS90126.1), CYP82F1_ARALY (EFH56916.1), CYP82X1_PAPSO (AFB74614.1), CYP82X2_PAPSO (AFB74616.1), CYP82Y1 (AFB74617.1), P6H_ESCCA (F2Z9C1.1), P6H_PAPSO (L7X0L7.1), and MSH_PAPSO (L7X3S1.1)

Oxidoreductases: COR13_PAPSO (Q9SQ68.1), COR14_PAPSO (Q9SQ67.2), COR12_PAPSO (Q9SQ69.1), COR11_PAPSO (Q9SQ70.1), COR15_PAPSO (B9VRJ2.1), COR2_PAPSO (Q9SQ64.1), PKR1_GLYGL (BAA13113.1), CR_MEDSA (Q40333), 6DCS_SOYBN (P26690.1), GALUR_FRAAN (O49133.1), NADO2_ORYSJ (Q7G765.1), NADO1_ORYSJ (Q7G764.1), MER_ERYCB (E7C196.1), CR_SESRO (CAA11226.1), AKRCA_ARATH (Q84TF0.1), AKRC9_ARATH (Q0PGJ6.1), AKRCB_ARATH (Q9M338.1), CAC32834_DIGPU (CAC32834.1), CAC32835_DIGPU (CAC32835.1), AKRC8_ARATH (O80944.2), S6PD_MALDO (P28475.1), and ALDR_HORVU (P23901.1).

All amino acid sequences were aligned with ClustalX and the alignments were reconciled and further adjusted by eye to minimize insertion/deletion events. Only the most conserved residues in the alignment regions were used in the subsequent phylogenetic analyses. Distance analyses used the Protdist program with a Jones-Taylor-Thornton substitution matrix of the Phylip 3.6b package (*42*). Phylogenetic trees were calculated from the distance matrices by the neighbour-joining algorithm. Bootstrap analyses consisted of 1000 replicates using the same protocol. Groups with above 70% bootstrap value were considered as strongly supported (Fig. S5).

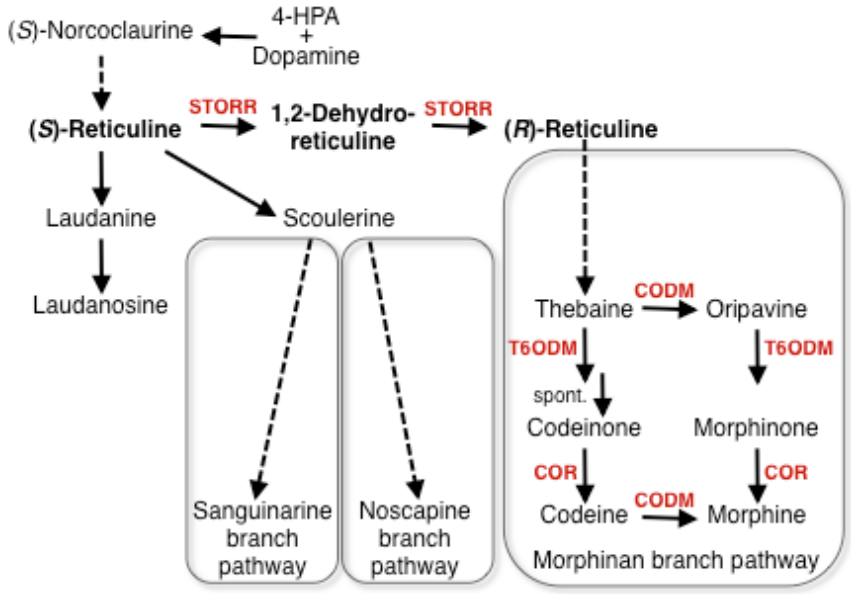

Fig. S1

Schematic overview of BIA metabolism depicting the central role of reticuline epimerization. Broken lines denote multiple enzymatic steps. 4-HPA - 4-hydroxyphenylacetaldehyde, CODM - codeine O-demethylase, T6ODM - thebaine 6-O-demethylase, COR – codeinone reductase

ATGGAGCTCCAATATATTTCTTATTTTCAACCAACTTCCTCCGTTGTTGCTCTTCTACTTGCTCTTGTATC
CATCTTATCCAGTGTCGTTGTTTTGAGGAAGACATTTTTGAATAACTACTCATCATCACCTGCATCATCCA
CAAAAACAGCGGTACTTTCTCATCAGCGGCAGCAGTCGTGTGCATTGCCAATTTCCGGTCTCCTCCATATT
TTCATGAATAAAAACGGCTTAATTCATGTAACTCTTGGAAATATGGCTGATAAATACGGTCCGATTTTCAG
TTTCCCAACAGGTAGCCATAGAACTCTCGTTGTGAGCAGTTGGGAGATGGTAAAAGAGTGTTTTACTGGCA
ACAATGACACTGCTTTCTCAAACCGTCCTATCCCGTTAGCTTTTAAGACTATATTCTATGCATGCGGTGGC
ATAGACTCATACGGTCTTTCGAGTGTACCTTATGGAAAATATTGGAGGGAGCTTCGAAAGGTCTGTGTGCA
TAACCTCCTGTCTAATCAACAACTACTCAAGTTCAGACACTTGATAATTTCTCAAGTCGATACGTCTTTCA
ATAAGCTGTATGAGTTATGCAAAAACTCTGAAGACAACCATGGAAACTATACTACTACTACTACTACCGCA
GCTGGCATGGTGAGAATCGATGATTGGCTCGCCGAATTATCGTTCAATGTGATAGGAAGAATAGTCTGCGG
ATTCCAATCAGGCCCTAAGACAGGTGCTCCAAGCAGGGTGGAACAATTTAAAGAAGCAATTAATGAAGCAT
CTTATTTTATGTCGACATCTCCAGTGTCAGATAATGTTCCAATGCTAGGGTGGATTGACCAATTGACAGGT
CTTACGAGAAATATGAAGCACTGCGGAAAGAAATTAGACTTGGTGGTCGAGAGCATAATTAATGATCATCG
TCAAAAGAGACGATTCTCTAGAACTAAAGGAGGAGATGAGAAGGACGATGAACAAGATGACTTCATCGACA
TTTGTTTGTCAATAATGGAGCAACCACAGCTTCCTGGCAACAATAATCCTTCTCAGATACCTATCAAATCT
ATTGTCCTGGACATGATAGGTGGGGGCACTGACACCACAAAACTGACCACCATCTGGACCCTTTCCTTGCT
GCTGAACAACCCCCATGTGTTGGACAAGGCAAAACAAGAAGTGGATGCACACTTTCGAACCAAAAGGAGAT
CAACAAATGATGCAGCAGCAGCCGTGGTGGATTTTGATGATATTCGTAACCTTGTCTACATCCAGGCAATC
ATCAAAGAATCAATGCGGTTGTATCCAGCCAGCCCCGTGGTGGAGCGACTGAGCGGCGAAGATTGTGTGGT
CGGTGGGTTTCATGTACCAGCAGGGACGAGATTATGGGCTAACGTATGGAAGATGCAACGAGACCCTAAAG
TATGGGATGATCCATTGGTGTTTCGACCAGACAGATTTTTGAGCGATGAACAGAAGATGGTTGATGTAAGG
GGTCAAAATTATGAGCTGTTACCATTTGGAGCCGGTCGACGTGTATGTCCAGGTGTATCCTTCTCTTTGGA
TCTAATGCAACTGGTACTGACTCGTCTTATTCTCGAGTTTGAAATGAAGTCTCCTAGCGGGAAAGTGGACA
TGACAGCAACACCAGGATTAATGAGTTACAAGGTGATCCCCCTTGACATTCTGCTCACCCATCGTCGCATA
*AAGCCGTGTGTGCAGTCAGCAGCCTCTGAGAGAGAC*ATGGAGAGTAGTGGTGTACCAGTAATCACTCTGGG
CTCGGGCAAGGTGATGCCTGTTCTTGGCATGGGAACATTTGAGAAAGTTGGTAAAGGGTCCGAAAGAGAGA
GGTTGGCGATTTTAAAAGCGATAGAGGTGGGTTACAGATACTTCGATACAGCTGCTGCATACGAAACTGAA
GAGGTTCTTGGAGAAGCTATTGCTGAAGCACTTCAACTTGGCCTAGTCAAATCTCGAGATGAACTTTTCAT
CAGTTCCATGCTCTGGTGCACTGATGCTCACGCTGATCGTGTCCTCCTCGCTCTTCAGAATTCGCTGAGGA
ATCTTAAATTGGAGTATGTGGATCTATATATGTTACCCTTCCCGGCAAGCTTGAAGCCTGGGAAGATAACG
ATGGACATACCAGAGGAAGATATTTGTCGCATGGACTACAGGTCTGTATGGGCAGCCATGGAAGAGTGTCA
AAACCTTGGCTTCACTAAATCAATCGGTGTTAGCAATTTCTCCTGCAAAAAGCTTCAGGAATTGATGGCGA
CTGCCAACATCCCTCCAGCTGTGAATCAAGTGGAGATGAGCCCGGCTTTCCAACAAAAGAAGCTGAGAGAG
TATTGCAACGCAAATAATATATTAGTCAGTGCAATCTCTGTACTGGGATCAAACGGAACCCCATGGGGCTC
CAATGCAGTTTTGGGTTCTGAGGTGCTTAAGAAAATTGCTATGGCCAAAGGAAAATCTGTTGCTCAGGTTA
GTATGAGATGGGTTTACGAGCAAGGCGCGAGTCTTGTGGTAAAAAGTTTCAGTGAAGAGAGATTGAGGGAA
AACTTGAACATATTTGACTGGGAACTCACTAAGGAAGACCATGAAAAGATCGGTGAGATTCCACAGTGCAG
AATCTTGAGTGCTTATTTTTTGGTCTCACCTAATGGACCTTTCAAATCTCAAGAAGAGTTGTGGGATGATG
AAGCTTGAAACATCGATCACTTAACTCTAGACATGCATTTATAAGAGAAGCTTCCCCTGCTGTGTGCTCAA
TCTTGATTTATTTTATCAAATTACATCTTGCTATAAGGGAGTCACGGATCTCATTCCCTTC

Fig. S2
Full-length *STORR* cDNA sequence.

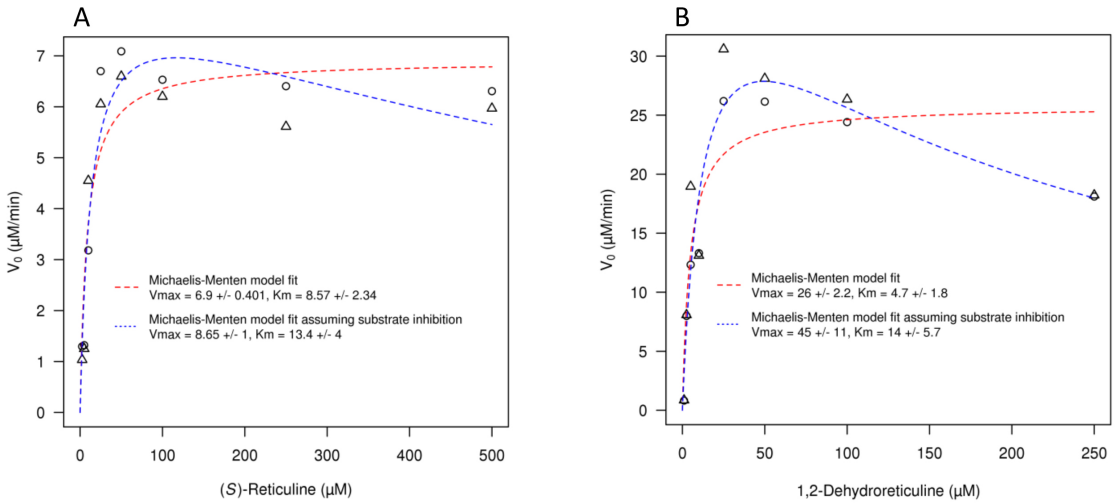

Fig. S3

Enzyme kinetics for microsomally-expressed proteins. Microsomal enzyme preparations for the N-terminal CYP82Y2 (A) and the full-length STORR (CYP82Y2-Oxired) (B) protein were incubated over a range of substrate concentrations (1 – 500 µM) and reaction times (1 – 30 min). Initial rates (V_0) were calculated from progress curves (*38*), and reaction kinetics were modeled using non-linear regression with the nls function available in R (*39*). Michaelis-Menten models were fitted using the terms:

$$V_0 = (Vmax * [S]) / (Km + [S])$$

or, assuming substrate inhibition:

$$V_0 = (Vmax * [S]) / (Km + [S]) * (1 + S/Ks)$$

In each case, experiments were performed in duplicate (different symbols) and models fitted to all the data. Km and Vmax values are expressed in units of µM and µM/min, respectively.

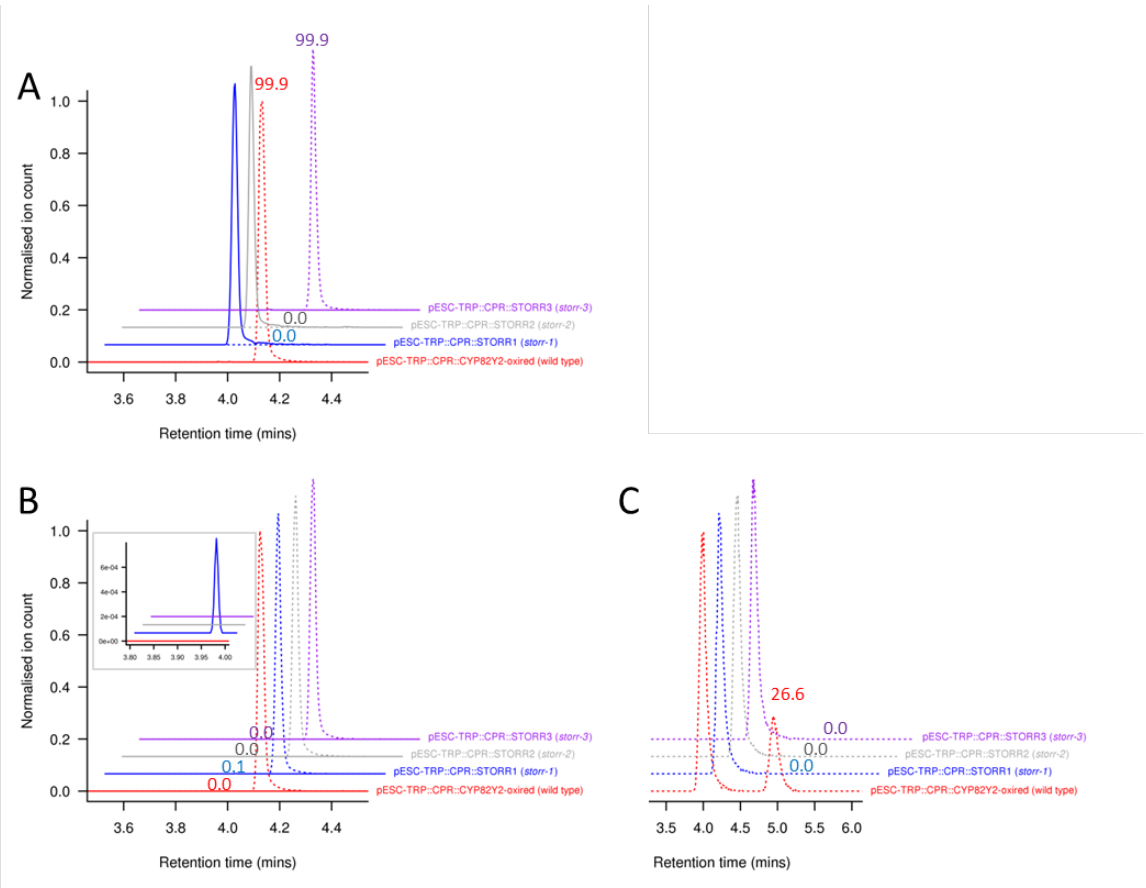

Fig. S4

Activity evaluation of heterologously expressed mutant proteins. Mutant proteins were expressed in *S. cerevisiae* and microsomal end-point assays performed as described in the methods. Relevant substrates (100 µM) were fed to microsomal preparations containing 4 – 10 mg protein equivalents over 3h. 1,2-dehydroreticuline and (*SR*)-reticuline were determined using the trifluoroacetic acid based HPLC-MS method. The proportion of reticuline epimers was determined using the chiral LCMS method. Results are displayed as described in Fig. 3, with panels (A) and (B) showing non-chiral analyses of samples fed 1,2- dehydroreticuline (retention time ~ 3.9 min) or (*S*)-reticuline ((*SR*)-reticuline retention time ~ 4.1 min), respectively. Panel (C) shows chiral analysis of samples fed (*S*)-reticuline (retention time ~ 4.0 min; (*R*)-reticuline ~ 5.0 min). Percent conversions were calculated as proportions of summed peak areas at the end of the assay and are printed above the expected product peak retention times. The low percentage conversion of (*S*)-reticuline to 1,2-dehydroreticuline observed in the *storr-1* mutant protein assay (Panel B; blue trace and inset) is consistent with the low levels of this compound detected *in-planta* for this mutant.

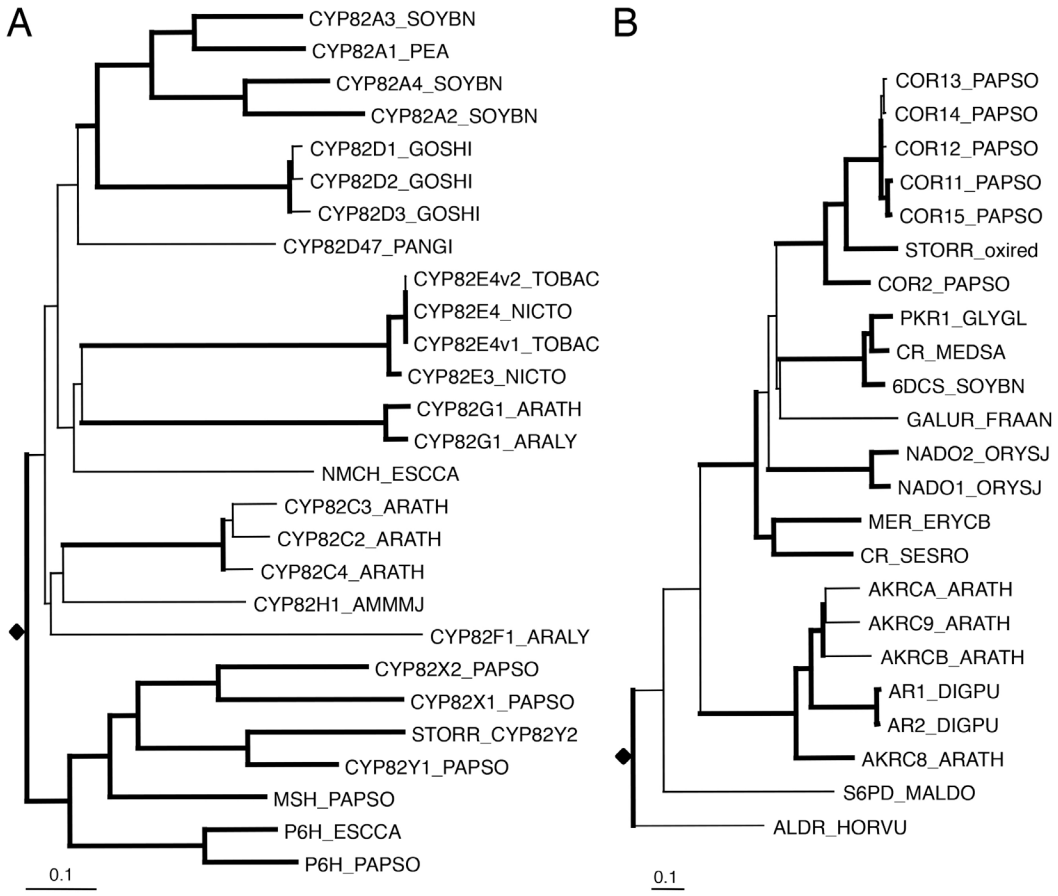

Fig. S5

Phylogenetic analysis of the cytochrome P450 and oxidoreductase modules of the STORR protein from *Papaver somniferum*. (A) N-terminal cytochrome P450 module (STORR_CYP82Y2) together with other cytochrome P450 proteins in the CYP82 subfamily. (B) C-terminal oxidoreductase module (STORR_oxired) with proteins of the aldo/keto-reductase 4 family.

Species-specific identifiers: *Ammi majus* (_AMMMJ), *Arabidopsis lyrata* (_ARALY*), Arabidopsis thaliana* (_ARATH), *Digitalis purpurea* (_DIGPU), *Erythroxylum coca* (_ERYCB), *Eschscholzia californica* (_ESCCA), *Fragaria x ananassa* (_FRAAN), *Glycyrrhiza glabra* (_GLYGL), *Gossypium hirsutum* (_GOSHI), *Glycine max* (_SOYBN), *Hordeum vulgare* (_HORVU), *Malus domestica* (_MALDO), *Medicago sativa* (_MEDSA), *Nicotiana tabacum* (_TOBAC), *Nicotiana tomentosiformis* (_NICTO), *Oryza sativa* Japonica (_ORYSJ), *Panax ginseng* (_PANGI), *Papaver somniferum* (_PAPSO), *Pisum sativum* (_PEA), *Sesbania rostrata* (_SESRO).

Abbreviations: *N*-methylcoclaurine 3'-hydroxylase (NMCH), *N*-methylstylopine 14-hydroxylase (MSH), protopine 6-hydroxylase (P6H), codeinone reductase (COR), polyketide reductase (PKR), chalcone reductase (CR),

6'-deoxychalcone synthase (6DCS), galacturonate reductase (GALUR), NAD(P)H-dependent oxidoreductase (NADO), Methylecgonone reductase (MER), aldo-keto reductase (AKR), sorbitol-6-phosphate dehydrogenase (S6PD), aldehyde reductase (ALDR).
All branches are drawn to scale as indicated by the scale bar (0.1 substitutions/site). The solid diamonds indicate the root of the phylogenetic trees. Strongly supported nodes with above 70% bootstrap values are highlighted with thickened lines.

ATGGGTTCAAACAACTTAGCCAACTCAATAGAATCAATGTTAGGTATCTCAATAGGTTCAGAATACATCTC
CGATCCAATCTTTATCATGGTCACTACAGTTGCTTCCATGTTAATTGGTTTTGGTTTCTTTGCATGTATGA
AATCTTCATCCAGTCAATCTAAGCCAATCGAAACTTACAAGCCTATCATCGACAAGGAAGAAGAAGAAATC
GAAGTTGATCCAGGTAAAATTAAATTGACAATCTTTTTCGGTACACAAACCGGTACTGCAGAAGGTTTTGC
CAAAGCTTTGGCAGAAGAAATTAAAGCAAAGTACAAAAAGGCCGTTGTAAAGGTCGTTGATTTGGATGACT
ATGCTGCAGAAGATGACCAATACGAAGAAAAGTTGAAAAAGGAATCTTTGGTTTTCTTTATGGTAGCTACA
TATGGTGACGGTGAACCTACCGATAATGCCGCTAGATTTTACAAGTGGTTCACACAAGAACATGAACGTGG
TGAATGGTTGCAACAATTAACCTATGGTGTTTTTGGTTTGGGTAACAGACAATACGAACACTTCAACAAAA
TTGCAGTCGACGTTGATGAACAATTGGGTAAACAAGGTGCTAAGAGAATAGTACAAGTCGGTTTAGGTGAC
GACGATCAATGTATCGAAGACGATTTTACTGCTTGGAGAGAATTGTTGTGGACAGAATTGGATCAATTGTT
GAAGGACGAAGATGCAGCCCCATCTGTTGCTACCCCTTATATTGCAACTGTACCAGAATACAGAGTAGTCA
TACATGAAACCACTGTTGCTGCATTGGACGATAAACACATTAATACTGCCAACGGTGACGTTGCTTTCGAT
ATCTTGCATCCATGTAGAACAATCGTAGCTCAACAAAGAGAATTGCATAAGCCTAAGAGTGATAGATCTTG
CATCCACTTGGAATTCGATATCTCTGGTTCTTCATTGACATACGAAACCGGTGACCATGTTGGTGTATACG
CCGAAAACTGTGATGAAACCGTTGAAGAAGCTGGTAAATTGTTGGGTCAACCATTGGATTTGTTATTTTCA
ATACACACAGACAAGGAAGATGGTTCCCCTCAAGGTTCCAGTTTGCCACCTCCATTCCCTGGTCCATGCAC
TTTGAGATCTGCCTTAGCTAGATATGCAGATTTGTTAAATCCTCCAAGAAAAGCTTCATTGATAGCATTAT
CCGCACATGCCTCAGTTCCATCCGAAGCTGAAAGATTGAGATTTTTATCTTCACCTTTGGGTAAAAACGAA
TACTCTAAGTGGGTTGTAGGTAGTCAAAGATCTTTGTTAGAAATCATGGCAGAATTCCCATCAGCCAAACC
TCCATTGGGTGTTTTCTTTGCCGCTGTAGCTCCTAGATTACCTCCAAGATATTACTCCATCTCCAGTTCTC
CAAAGTTTGCACCTAGTAGAATTCATGTCACATGTGCCTTGGTTTATGGTCAATCTCCAACCGGTAGAGTC
CATAGAGGTGTTTGCTCAACTTGGATGAAACACGCCGTCCCACAAGATAGTTGGGCTCCTATATTCGTTAG
AACTTCTAACTTCAAGTTGCCTGCTGATCCATCAACCCCTATCATTATGGTTGGTCCAGGTACTGGTTTAG
CACCTTTTAGAGGTTTCTTGCAAGAAAGAATGGCCTTAAAAGAAAACGGTGCTCAATTGGGTCCAGCAGTT
TTATTTTTCGGTTGTAGAAACAGAAACATGGACTTCATCTATGAAGATGAATTGAACAACTTCGTAGAAAG
AGGTGTCATTAGTGAATTAGTTATAGCATTTTCTAGAGAAGGTGAAAAGAAAGAATACGTTCAACATAAGA
TGATGGAAAAGGCTACAGACGTATGGAATGTCATCTCTGGTGACGGTTATTTGTACGTATGCGGTGACGCC
AAGGGTATGGCTAGAGATGTCCATAGAACTTTACACACAATTGCTCAAGAACAAGGTCCAATGGAATCATC
CGCAGCCGAAGCTGCAGTTAAGAAATTGCAAGTCGAAGAAAGATATTTGAGAGATGTTTGGTAA

Fig. S6

Yeast codon optimized PsCPR

ATGGAATTACAATACATCTCCTACTTTCAACCAACCTCTTCAGTCGTCGCTTTGTTATTAGCATTAGTCTC
TATCTTATCCTCCGTAGTTGTATTGAGAAAGACATTTTTGAACAACTACTCTTCATCCCCAGCCAGTTCTA
CAAAGACCGCTGTTTTGTCACATCAAAGACAACAATCCTGTGCTTTGCCTATCAGTGGTTTGTTGCATATA
TTCATGAACAAAAACGGTTTGATCCACGTTACATTGGGTAATATGGCTGATAAGTACGGTCCAATCTTTAG
TTTCCCTACAGGTTCTCACAGAACCTTGGTCGTTTCATCCTGGGAAATGGTTAAGGAATGCTTCACTGGTA
ACAACGATACAGCTTTCTCAAATAGACCAATACCTTTAGCCTTTAAGACTATCTTCTATGCTTGTGGTGGT
ATTGATTCCTACGGTTTGAGTTCTGTTCCATACGGTAAATACTGGAGAGAATTGAGAAAGGTCTGCGTTCA
TAACTTGTTGTCTAACCAACAATTGTTGAAGTTTAGACACTTGATTATATCACAAGTTGACACATCCTTCA
ACAAATTGTACGAATTGTGTAAGAACTCTGAAGATAACCATGGTAACTACACTACAACCACTACAACCGCT
GCTGGTATGGTTAGAATTGATGACTGGTTGGCTGAATTGTCTTTTAATGTTATCGGTAGAATCGTATGCGG
TTTCCAATCAGGTCCAAAAACTGGTGCACCTTCCAGAGTTGAACAATTCAAAGAAGCAATTAACGAAGCCA
GTTATTTCATGTCAACATCCCCAGTCTCTGACAATGTTCCTATGTTAGGTTGGATTGATCAATTGACCGGT
TTGACTAGAAACATGAAGCATTGTGGTAAAAAGTTGGACTTGGTAGTCGAATCAATCATTAATGATCACAG
ACAAAAGAGAAGATTTTCCAGAACTAAAGGTGGTGACGAAAAGGATGACGAACAAGATGACTTCATCGATA
TCTGCTTGTCAATCATGGAACAACCACAATTACCTGGTAACAACAACCCATCTCAAATCCCTATTAAATCA
ATCGTTTTGGACATGATTGGTGGTGGTACTGATACTACAAAGTTGACCACTATATGGACATTGTCTTTGTT
GTTGAACAACCCACATGTCTTAGACAAAGCAAAGCAAGAAGTTGATGCCCACTTTAGAACCAAAAGAAGAT
CTACTAACGACGCCGCTGCAGCCGTTGTAGATTTCGATGACATCAGAAATTTGGTTTACATCCAAGCCATA
ATCAAGGAATCCATGAGATTGTACCCAGCTAGTCCTGTCGTTGAAAGATTATCTGGTGAAGATTGTGTAGT
CGGTGGTTTTCATGTACCAGCTGGTACTAGATTATGGGCAAACGTCTGGAAAATGCAAAGAGATCCTAAGG
TTTGGGATGACCCATTGGTTTTTAGACCTGATAGATTCTTATCAGACGAACAAAAGATGGTAGATGTCAGA
GGTCAAAACTACGAATTGTTGCCATTCGGTGCTGGTAGAAGAGTATGTCCTGGTGTCAGTTTCTCTTTGGA
TTTGATGCAATTAGTTTTGACCAGATTGATATTGGAATTCGAAATGAAGTCACCATCCGGTAAAGTTGATA
TGACTGCTACACCAGGTTTGATGTCTTACAAAGTAATCCCTTTGGATATCTTGTTGACACATAGAAGAATT
AAACCATGCGTTCAATCAGCTGCATCCGAAAGAGATATGGAATCATCCGGTGTTCCAGTAATCACCTTGGG
TTCTGGTAAAGTCATGCCTGTTTTGGGTATGGGTACTTTTGAAAAAGTTGGTAAAGGTTCCGAAAGAGAAA
GATTGGCTATATTAAAGGCAATCGAAGTAGGTTATAGATACTTCGATACAGCCGCTGCATATGAAACCGAA
GAAGTCTTGGGTGAAGCAATTGCCGAAGCTTTGCAATTGGGTTTAGTTAAATCTAGAGATGAATTGTTTAT
AAGTTCTATGTTGTGGTGTACTGATGCACACGCCGACAGAGTATTGTTGGCTTTGCAAAACAGTTTGAGAA
ATTTGAAGTTGGAATATGTCGATTTGTACATGTTACCATTTCCTGCATCTTTGAAGCCAGGTAAAATCACA
ATGGATATCCCTGAAGAAGACATCTGTAGAATGGATTACAGAAGTGTTTGGGCCGCTATGGAAGAATGCCA
AAACTTAGGTTTTACAAAGTCTATCGGTGTTAGTAACTTCTCTTGTAAAAAGTTGCAAGAATTAATGGCTA
CCGCAAACATTCCACCTGCTGTAAATCAAGTCGAAATGTCACCAGCATTCCAACAAAAGAAATTGAGAGAA
TACTGCAATGCAAACAATATATTGGTCTCAGCCATCTCCGTTTTAGGTTCTAACGGTACTCCTTGGGGTTC
CAATGCTGTATTGGGTAGTGAAGTCTTGAAGAAAATTGCCATGGCTAAAGGTAAAAGTGTTGCACAAGTAT
CTATGAGATGGGTTTATGAACAAGGTGCCTCTTTGGTTGTAAAGAGTTTTTCTGAAGAAAGATTGAGAGAA
AACTTAAACATCTTCGACTGGGAATTGACAAAGGAAGATCATGAAAAGATTGGTGAAATACCACAATGTAG
AATATTGTCTGCTTACTTTTTAGTTTCACCAAATGGTCCTTTCAAATCTCAAGAAGAATTATGGGATGACG
AAGCATAA

Fig. S7
Yeast codon optimized STORR (CYP82Y2-oxired)

ATGGAATTACAATACATTTCTTACTTTCAACCTACATCCTCTGTCGTCGCCTTGTTATTAGCATTAGTCTC
TATCTTATCCTCCGTCGTTGTATTGAGAAAGACATTTTTGAACAACTACTCTTCATCCCCAGCAAGTTCTA
CAAAGACCGCCGTTTTATCACATCAAAGACAACAATCCTGTGCTTTGCCTATAAGTGGTTTGTTGCATATC
TTTATGAACAAAAACGGTTTGATCCACGTAACATTGGGTAATATGGCTGATAAGTACGGTCCAATTTTCTC
TTTCCCTACAGGTTCCCACAGAACCTTAGTCGTTTCATCCTGGGAAATGGTTAAGGAATGCTTCACTGGTA
ACAACGATACAGCTTTCAGTAATAGACCAATCCCTTTGGCTTTTAAAACTATTTTCTATGCCTGTGGTGGT
ATAGATTCTTACGGTTTAAGTTCTGTTCCATATGGTAAATACTGGAGAGAATTGAGAAAGGTTTGCGTACA
TAACTTGTTATCAAATCAACAATTGTTGAAGTTTAGACACTTAATAATCAGTCAAGTTGATACATCTTTCA
ACAAATTATATGAATTGTGTAAGAATTCTGAAGACAACCATGGTAATTACACTACAACCACTACAACCGCT
GCTGGTATGGTTAGAATTGATGACTGGTTAGCCGAATTGTCTTTTAATGTCATAGGTAGAATCGTTTGCGG
TTTCCAATCAGGTCCAAAAACTGGTGCACCTTCCAGAGTTGAACAATTCAAAGAAGCCATAAACGAAGCTA
GTTATTTCATGTCAACATCCCCAGTATCTGATAATGTCCCTATGTTGGGTTGGATTGACCAATTAACCGGT
TTGACTAGAAACATGAAGCATTGTGGTAAAAAGTTGGATTTGGTAGTCGAATCAATCATTAATGACCACAG
ACAAAAGAGAAGATTTTCCAGAACTAAAGGTGGTGACGAAAAGGATGACGAACAAGATGACTTCATCGACA
TCTGCTTGTCTATCATGGAACAACCACAATTGCCTGGTAACAACAACCCATCTCAAATCCCTATTAAATCA
ATCGTTTTGGATATGATTGGTGGTGGTACAGACACTACAAAGTTAACCACTATTTGGACCTTGTCATTGTT
GTTGAACAACCCACATGTTTTGGATAAGGCTAAGCAAGAAGTAGACGCACACTTTAGAACCAAAAGAAGAT
CCACTAACGATGCCGCTGCAGCCGTTGTAGACTTCGATGACATAAGAAATTTGGTTTACATCCAAGCTATA
ATCAAAGAATCCATGAGATTGTACCCAGCAAGTCCTGTCGTTGAAAGATTGTCTGGTGAAGATTGTGTAGT
CGGTGGTTTTCATGTCCCAGCCGGTACTAGATTGTGGGCTAACGTTTGGAAAATGCAAAGAGATCCTAAAG
TATGGGATGACCCATTAGTCTTTAGACCTGATAGATTCTTGTCTGACGAACAAAAGATGGTCGATGTTAGA
GGTCAAAACTACGAATTGTTGCCATTTGGTGCTGGTAGAAGAGTTTGTCCTGGTGTAAGTTTCTCTTTGGA
TTTGATGCAATTAGTTTTGACCAGATTGATATTGGAATTCGAAATGAAGTCACCATCCGGTAAAGTAGATA
TGACTGCTACACCAGGTTTAATGTCTTACAAAGTCATTCCTTTGGATATCTTGTTGACACATAGAAGAATT
AAGCCATGCGTTCAAAGTGCTGCATCTGAAAGAGATTAA

Fig. S8
Yeast codon optimized CYP82Y2 module

ATGGAATCCTCTGGTGTCCCTGTTATCACATTGGGTTCTGGTAAAGTTATGCCTGTCTTGGGTATGGGTAC
ATTTGAAAAGGTCGGTAAAGGTTCTGAAAGAGAAAGATTAGCCATCTTGAAGGCTATTGAAGTTGGTTATA
GATACTTTGACACTGCTGCAGCCTATGAAACAGAAGAAGTATTAGGTGAAGCCATCGCTGAAGCATTGCAA
TTAGGTTTGGTCAAGTCTAGAGATGAATTATTCATTTCTTCAATGTTGTGGTGTACAGATGCCCATGCTGA
CAGAGTTTTGTTAGCTTTGCAAAACTCTTTGAGAAACTTAAAGTTGGAATACGTAGATTTGTACATGTTGC
CATTTCCTGCTTCATTGAAGCCAGGTAAAATCACCATGGATATCCCTGAAGAAGACATATGTAGAATGGAT
TACAGATCCGTTTGGGCTGCAATGGAAGAATGCCAAAATTTGGGTTTTACCAAGAGTATCGGTGTTTCTAA
CTTCTCATGTAAAAAGTTGCAAGAATTGATGGCAACTGCCAATATCCCACCTGCTGTCAACCAAGTTGAAA
TGTCCCCAGCATTCCAACAAAAGAAATTGAGAGAATACTGCAACGCAAACAACATTTTAGTTTCCGCCATA
AGTGTATTGGGTTCAAATGGTACTCCTTGGGGTTCCAACGCTGTCTTAGGTAGTGAAGTTTTGAAAAAGAT
TGCTATGGCAAAGGGTAAATCTGTAGCCCAAGTCTCAATGAGATGGGTTTATGAACAAGGTGCATCATTAG
TTGTAAAATCCTTTAGTGAAGAAAGATTGAGAGAAAATTTGAACATATTCGACTGGGAATTGACAAAAGAA
GATCACGAAAAGATTGGTGAAATACCACAATGCAGAATCTTGTCTGCTTACTTTTTGGTTTCACCAAATGG
TCCTTTCAAGTCTCAAGAAGAATTGTGGGATGACGAAGCATAA

Fig. S9

Yeast codon optimized oxidoreductase (oxired) module

Table S1

Reticuline epimers in *storr* mutants. (*S*)- and (*R*)-reticuline epimers were resolved by chiral HPLC as described in the methods and the $[M+H]^+$ pseudomolecular ion at m/z 330.17 used to quantify each epimer.

Mutation	Plant	Peak Areas		Epimer composition (%)	
		(*S*)-Reticuline	(*R*)-Reticuline	(*S*)-Reticuline	(*R*)-Reticuline
storr-1	1	193951969	228894	99.88	0.12
	2	78769877	123097	99.84	0.16
	3	203130725	404437	99.80	0.20
	4	190190017	418958	99.78	0.22
	5	86282424	203210	99.77	0.23
	6	190124212	472528	99.75	0.25
	7	84069601	225883	99.73	0.27
	8	51997079	142964	99.73	0.27
	9	206014385	857515	99.59	0.41
	10	83810777	427471	99.49	0.51
	11	67295542	436143	99.36	0.64
	12	178730687	1308507	99.27	0.73
	mean	134530608	437467	99.67	0.33
	SD	62796474	339334	0.20	0.20
storr-2	1	520359208	251005	99.95	0.05
	2	370727515	241554	99.93	0.07
	3	108897212	79229	99.93	0.07
	4	154134338	126075	99.92	0.08
	5	289659860	238567	99.92	0.08
	6	114540297	114693	99.90	0.10
	7	348519342	351006	99.90	0.10
	8	105038247	121516	99.88	0.12
	9	526976855	678815	99.87	0.13
	10	191487938	250501	99.87	0.13
	11	172226213	277557	99.84	0.16
	12	155844498	252069	99.84	0.16
	13	235645412	484513	99.79	0.21
	14	127590915	310733	99.76	0.24
	15	125500009	563301	99.55	0.45
	16	132278512	695276	99.48	0.52
	17	102549230	583898	99.43	0.57
	mean	222469153	330606	99.81	0.19
	SD	140505956	198515	0.16	0.16
storr-3	1	679690881	219435	99.97	0.03
	2	376570063	186977	99.95	0.05
	3	274171284	213661	99.92	0.08
	4	416724371	339626	99.92	0.08
	5	132344291	126899	99.90	0.10
	6	297068936	307636	99.90	0.10
	7	306622485	325573	99.89	0.11
	8	232824354	269834	99.88	0.12
	9	476240726	573810	99.88	0.12
	10	78300200	119211	99.85	0.15
	11	184559563	305635	99.83	0.17
	12	258032848	438033	99.83	0.17
	13	240979799	629862	99.74	0.26
	14	199605477	530382	99.73	0.27
	15	469154205	1352617	99.71	0.29
	mean	308192632	395946	99.86	0.14
	SD	154332995	306876	0.08	0.08

Table S2

Combined genotype and phenotype analysis of individuals from F2 populations segregating for *storr* alleles. Genotyping and phenotyping was carried out as described in materials and methods. Alkaloids were measured in dried capsules in the case of F2 population S-110753 segregating for *storr-1* or stem latex in case of F2 populations S-110756 and S-110744 segregating for *storr-2* and *storr-3* respectively.
M = morphine, C = codeine, O = oripavine, T = thebaine, N = noscapine, R = reticuline; DW = dry weight; WT = homozygous for *STORR* wild type allele, Het = heterozygous, Hom = homozygous for *Storr* mutant allele.

Mutant allele	F2 population	Genotype	% capsule DW					
			M	**C**	**O**	**T**	**N**	**R**
storr-1	S-110753 n =55	WT n = 12	2.66 ± 0.47	0.065 ± 0.05	0.000	0.014 ± 0.02	1.8 ± 0.09	0.006 ± 0.002
		Het n = 29	3.37 ± 0.58	0.14 ± 0.08	0.005 ± 0.006	0.039 ± 0.05	0.2 ± 0.09	0.063 ± 0.021
		Hom n = 14	0.01 ± 0.001	0.1 ± 0.03	0.000	0.000	0.000	0.89 ± 0.22
			% of total alkaloid peak area					
			M	**C**	**O**	**T**	**N**	**R**
storr-2	S-110756 n = 15	WT n = 6	26.0 ± 13.2	11.1 ± 5.1	1.2 ± 0.8	56.1 ± 14.4	0.0	0.8 ± 0.3
		Het n = 4	10.7 ± 7.0	23.2 ± 18.6	0.3 ± 0.3	40.5 ± 15.1	0.0	12.3 ± 3.1
		Hom n = 5	0.5 ± 1.0	0.1 ± 0.1	0.04 ± 0.08	0.6 ± 1.2	0.0	72.5 ± 2.0
storr-3	S-110744 n = 19	WT n = 8	39.3 ± 11.2	24.3 ± 12.4	0.8 ± 0.7	27.2 ± 10.3	0.0	0.6 ± 0.3
		Het n = 4	41.3 ± 6.5	20 ± 10.3	0.4 ± 0.3	16.0 ± 9.8	0.0	6.9 ± 1.2
		Hom n = 7	0.2 ± 0.1	0.1 ± 0.03	0.0	0.1 ± 0.04	0.0	65.1 ± 3.1

Table S3
Complementation tests of *storr* mutants.
Relative peak areas (as a percentage of total peak-area) were calculated from LCMS chromatographic data (TFA method) obtained from 10 day old F1 seedlings. Complementation tests showed that the wild type HM2 phenotype was not rescued in the F1 of any of the possible *storr* mutant combinations. All F1s displayed the high reticuline phenotype and that of high (S)-reticuline derived non-morphinan alkaloids such as laudanine and laudanosine. Likewise, the high 1,2-dehydroreticuline phenotype displayed exclusively by *storr-1* was not rescued by crosses to *storr-2*. The high reticuline phenotype as well as that of (S)-reticuline derived non-morphinans was present in F1:storr-1×storr-3 but it is noteworthy that morphinans were also present albeit at a much reduced proportion (8.8%) compared to the HM2 wild type (97.7%). The occurrence of low levels of morphinans in F1:*storr-1×storr-3* is consistent with limited complementation occurring between the low activity CYP82Y2 module of *storr-1* and the active oxidoreductase module of *storr-3* (Table S4). However, the high reticuline phenotype in F1:*storr-1×storr-3* indicates that a major bottleneck at the STORR locus still exists. This could be due to the need to have both modules on the same polypeptide chain to facilitate efficient conversion of (*S*)- to (*R*)-reticuline, although steric consequences of the *storr-3* allele on the function of the oxidoreductase cannot be excluded.
The complementation analysis further corroborates the involvement of the *STORR* locus in the conversion of (*S*)- to (*R*)-reticuline with the CYP82Y2 module catalysing the formation of 1,2-dehydroreticuline from (*S*)-reticuline and the oxidoreductase module that of 1,2-dehydroreticuline to (*R*)-reticuline.

Genotype	Total Morphinans	Reticuline	1,2-Dehydroreticuline	non-Morphinan (*S*)-Reticuline derivatives*
HM2 (wild type)	97.7 (0.2)	1.4 (0.1)	0 (0)	0.9 (0.1)
storr-1	0 (0)	77.1 (0.6)	7.7 (0.4)	15.2 (1)
storr-2	0.7 (1.1)	71 (1.6)	0 (0)	28.2 (1.5)
storr-3	0 (0)	71.8 (4.6)	0 (0)	28.2 (4.6)
F1: *storr-1×storr-2*	0 (0)	73.2 (0.3)	5.2 (0.9)	21.5 (0.9)
F1: *storr-1×storr-3*	8.8 (0.6)	61.5 (1.8)	0 (0)	29.6 (1.3)
F1: *storr-3×storr-2*	0 (0)	68 (1.7)	0 (0)	32 (1.7)

*includes Laudanine, Laudanosine, Tetrahydropapaverine

Table S4

Contiguous assemblies encoding predicted P450-oxidoreductase fusions identified in the EST database of the 1K plant transcriptome project.

Blast searches were performed with the tblastn (*41*) algorithm using STORR protein as query sequence. Contiguous assemblies encoding highly similar predicted STORR homologues were identified in various organs of *P. setigerum* and *P. bracteatum* but not of *P. rhoeas*.

Species	Tissue	Contiguous assembly	Amino acid identity of predicted protein
Papaver somniferum	leaf	scaffold-BMRX-2007040	100%
Papaver setigerum	flower bud	scaffold-STDO-2019715	99% (899 out of 901 residues)
Papaver setigerum	stem	scaffold-MLPX-2016196	99% (899 out of 901 residues)
Papaver setigerum	developing fruit (capsule)	scaffold-EPRK-2027940	99% (899 out of 901 residues)
Papaver bracteatum	bulb	scaffold-TMWO-2027322	95% (854 out of 901 residues)
Papaver bracteatum	root	scaffold-ZSNV-2027701	95% (853 out of 901 residues)

REFERENCES

1. F. Sertürner, Darstellung der reinen Mohnsäure (Opiumsäure) nebst einer chemischen Untersuchung des Opiums. *J. der Pharmacie* **14**, 47 (1806).

2. Source: IMS Health Database (www.imshealth.com) (2013) Formulation sales by opiate molecule.

3. J. Ziegler, S. Voigtländer, J. Schmidt, R. Kramell, O. Miersch, C. Ammer, A. Gesell, T. M. Kutchan, Comparative transcript and alkaloid profiling in *Papaver* species identifies a short chain dehydrogenase/reductase involved in morphine biosynthesis. *Plant J.* **48**, 177–192 (2006). Medline doi:10.1111/j.1365-313X.2006.02860.x

4. M. Gates, G. Tschudi, The synthesis of morphine. *J. Am. Chem. Soc.* **78**, 1380–1393 (1956). Medline doi:10.1021/ja01588a033

5. N. Samanani, D. K. Liscombe, P. J. Facchini, Molecular cloning and characterization of norcoclaurine synthase, an enzyme catalyzing the first committed step in benzylisoquinoline alkaloid biosynthesis. *Plant J.* **40**, 302–313 (2004). Medline doi:10.1111/j.1365-313X.2004.02210.x

6. A. Ounaroon, G. Decker, J. Schmidt, F. Lottspeich, T. M. Kutchan, (*R,S*)-Reticuline 7-*O*-methyltransferase and (*R,S*)-norcoclaurine 6-*O*-methyltransferase of *Papaver somniferum* - cDNA cloning and characterization of methyl transfer enzymes of alkaloid biosynthesis in opium poppy. *Plant J.* **36**, 808–819 (2003). Medline doi:10.1046/j.1365-313X.2003.01928.x

7. K. B. Choi, T. Morishige, F. Sato, Purification and characterization of coclaurine *N*-methyltransferase from cultured *Coptis japonica* cells. *Phytochemistry* **56**, 649–655 (2001). Medline doi:10.1016/S0031-9422(00)00481-7

8. H. H. Pauli, T. M. Kutchan, Molecular cloning and functional heterologous expression of two alleles encoding (*S*)-N-methylcoclaurine 3′-hydroxylase (CYP80B1), a new methyl jasmonate-inducible cytochrome P-450-dependent mono-oxygenase of benzylisoquinoline alkaloid biosynthesis. *Plant J.* **13**, 793–801 (1998). Medline doi:10.1046/j.1365-313X.1998.00085.x

9. T. Morishige, T. Tsujita, Y. Yamada, F. Sato, Molecular characterization of the *S*-adenosyl-L-methionine:3′-hydroxy-N-methylcoclaurine 4′-*O*-methyltransferase involved in isoquinoline alkaloid biosynthesis in *Coptis japonica*. *J. Biol. Chem.* **275**, 23398–23405 (2000). Medline doi:10.1074/jbc.M002439200

10. A. Gesell, M. Rolf, J. Ziegler, M. L. Díaz Chávez, F. C. Huang, T. M. Kutchan, CYP719B1 is salutaridine synthase, the C-C phenol-coupling enzyme of morphine biosynthesis in opium poppy. *J. Biol. Chem.* **284**, 24432–24442 (2009). Medline doi:10.1074/jbc.M109.033373

11. R. Lenz, M. H. Zenk, Acetyl coenzyme A:salutaridinol-7-*O*-acetyltransferase from *Papaver somniferum* cell cultures: The enzyme catalyzing the formation of thebaine in morphine biosynthesis. *J. Biol. Chem.* **270**, 31091–31096 (1995). Medline doi:10.1074/jbc.270.52.31091

12. T. Grothe, R. Lenz, T. M. Kutchan, Molecular characterization of the salutaridinol 7-*O*-acetyltransferase involved in morphine biosynthesis in opium poppy *Papaver somniferum*. *J. Biol. Chem.* **276**, 30717–30723 (2001). Medline doi:10.1074/jbc.M102688200

13. J. M. Hagel, P. J. Facchini, Dioxygenases catalyze the O-demethylation steps of morphine biosynthesis in opium poppy. *Nat. Chem. Biol.* **6**, 273–275 (2010). Medline doi:10.1038/nchembio.317

14. B. Unterlinner, R. Lenz, T. M. Kutchan, Molecular cloning and functional expression of codeinone reductase: The penultimate enzyme in morphine biosynthesis in the opium poppy *Papaver somniferum*. *Plant J.* **18**, 465–475 (1999). Medline doi:10.1046/j.1365-313X.1999.00470.x

15. A. Nakagawa, H. Minami, J. S. Kim, T. Koyanagi, T. Katayama, F. Sato, H. Kumagai, A bacterial platform for fermentative production of plant alkaloids. *Nat. Commun.* **2**, 326 (2011). Medline doi:10.1038/ncomms1327

16. A. Nakagawa, C. Matsuzaki, E. Matsumura, T. Koyanagi, T. Katayama, K. Yamamoto, F. Sato, H. Kumagai, H. Minami, (R,S)-tetrahydropapaveroline production by stepwise fermentation using engineered *Escherichia coli*. *Sci Rep* **4**, 6695 (2014). Medline doi:10.1038/srep06695

17. K. M. Hawkins, C. D. Smolke, Production of benzylisoquinoline alkaloids in *Saccharomyces cerevisiae*. *Nat. Chem. Biol.* **4**, 564–573 (2008). Medline doi:10.1038/nchembio.105

18. K. Thodey, S. Galanie, C. D. Smolke, A microbial biomanufacturing platform for natural and semisynthetic opioids. *Nat. Chem. Biol.* **10**, 837–844 (2014). Medline doi:10.1038/nchembio.1613

19. W. De-Eknamkul, M. H. Zenk, Purification and properties of 1,2-dehydro-reticuline reductase from *Papaver somniferum* seedlings. *Phytochemistry* **31**, 813–821 (1992). doi:10.1016/0031-9422(92)80020-F

20. K. Hirata, C. Poeaknapo, J. Schmidt, M. H. Zenk, 1,2-Dehydroreticuline synthase, the branch point enzyme opening the morphinan biosynthetic pathway. *Phytochemistry* **65**, 1039–1046 (2004). Medline doi:10.1016/j.phytochem.2004.02.015

21. R. S. Allen, A. G. Millgate, J. A. Chitty, J. Thisleton, J. A. Miller, A. J. Fist, W. L. Gerlach, P. J. Larkin, RNAi-mediated replacement of morphine with the nonnarcotic alkaloid reticuline in opium poppy. *Nat. Biotechnol.* **22**, 1559–1566 (2004). Medline doi:10.1038/nbt1033

22. T. Winzer, V. Gazda, Z. He, F. Kaminski, M. Kern, T. R. Larson, Y. Li, F. Meade, R. Teodor, F. E. Vaistij, C. Walker, T. A. Bowser, I. A. Graham, A *Papaver somniferum* 10-gene cluster for synthesis of the anticancer alkaloid noscapine. *Science* **336**, 1704–1708 (2012). Medline doi:10.1126/science.1220757

23. Materials and methods are available as supplementary materials on *Science* Online.

24. F. P. Guengerich, A. W. Munro, Unusual cytochrome p450 enzymes and reactions. *J. Biol. Chem.* **288**, 17065–17073 (2013). Medline doi:10.1074/jbc.R113.462275

25. F. Brodhun, C. Göbel, E. Hornung, I. Feussner, Identification of PpoA from *Aspergillus nidulans* as a fusion protein of a fatty acid heme dioxygenase/peroxidase and a cytochrome P450. *J. Biol. Chem.* **284**, 11792–11805 (2009). Medline doi:10.1074/jbc.M809152200

26. B. G. Hansen, E. Mnich, K. F. Nielsen, J. B. Nielsen, M. T. Nielsen, U. H. Mortensen, T. O. Larsen, K. R. Patil, Involvement of a natural fusion of a cytochrome P450 and a hydrolase in mycophenolic acid biosynthesis. *Appl. Environ. Microbiol.* **78**, 4908–4913 (2012). Medline doi:10.1128/AEM.07955-11

27. I. Hoffmann, F. Jernerén, E. H. Oliw, Epoxy alcohol synthase of the rice blast fungus represents a novel subfamily of dioxygenase-cytochrome P450 fusion enzymes. *J. Lipid Res.* **55**, 2113–2123 (2014). Medline doi:10.1194/jlr.M051755

28. The thousand plant transcriptomes project (http://www.onekp.com).

29. S. C. Farrow, P. J. Facchini, Dioxygenases catalyze *O*-demethylation and *O,O*-demethylenation with widespread roles in benzylisoquinoline alkaloid metabolism in opium poppy. *J. Biol. Chem.* **288**, 28997–29012 (2013). Medline doi:10.1074/jbc.M113.488585

30. S. Chang, J. Puryear, J. Cairney, A simple and efficient method for isolating RNA from pine trees. *Plant Mol. Biol. Rep.* **11**, 113–116 (1993). doi:10.1007/BF02670468

31. D. Bonsor, S. F. Butz, J. Solomons, S. Grant, I. J. Fairlamb, M. J. Fogg, G. Grogan, Ligation independent cloning (LIC) as a rapid route to families of recombinant biocatalysts from sequenced prokaryotic genomes. *Org. Biomol. Chem.* **4**, 1252–1260 (2006). Medline doi:10.1039/b517338h

32. A. Rosco, H. H. Pauli, W. Priesner, T. M. Kutchan, Cloning and heterologous expression of NADPH-cytochrome P450 reductases from the Papaveraceae. *Arch. Biochem. Biophys.* **348**, 369–377 (1997). Medline doi:10.1006/abbi.1997.0374

33. D. Sorger, K. Athenstaedt, C. Hrastnik, G. Daum, A yeast strain lacking lipid particles bears a defect in ergosterol formation. *J. Biol. Chem.* **279**, 31190–31196 (2004). Medline doi:10.1074/jbc.M403251200

34. R. D. Geitz, R. A. Woods, in *Methods in Enzymology 350,* C. Guthrie, G. R. Fink, Eds. (Elsevier, 2002), vol. 350, pp. 87–96.

35. A. King, J. W. Nam, J. Han, J. Hilliard, J. G. Jaworski, Cuticular wax biosynthesis in petunia petals: Cloning and characterization of an alcohol-acyltransferase that synthesizes wax-esters. *Planta* **226**, 381–394 (2007). Medline doi:10.1007/s00425-007-0489-z

36. R. M. Horton, Z. L. Cai, S. N. Ho, L. R. Pease, Gene splicing by overlap extension: Tailor-made genes using the polymerase chain reaction. *Biotechniques* **8**, 528–535 (1990). Medline

37. K. Iwasa, Y. Doi, T. Takahashi, W. Cui, Y. Nishiyama, C. Tode, M. Moriyasu, K. Takeda, H. Minami, N. Ikezawa, F. Sato, Enantiomeric separation of racemic 1-benzyl-N-methyltetrahydroisoquinolines on chiral columns and chiral purity determinations of the O-methylated metabolites in plant cell cultures by HPLC-CD on-line coupling in

combination with HPLC-MS. *Phytochemistry* **70**, 198–206 (2009). Medline doi:10.1016/j.phytochem.2008.12.001

38. E. A. Boeker, Initial rates. A new plot. *Biochem. J.* **203**, 117–123 (1982). Medline

39. R Core Team, R: A language and environment for statistical computing. R Foundation for Statistical Computing, Vienna, Austria, http://www.R-project.org/ (2015).

40. S. F. Altschul, T. L. Madden, A. A. Schäffer, J. Zhang, Z. Zhang, W. Miller, D. J. Lipman, Gapped BLAST and PSI-BLAST: A new generation of protein database search programs. *Nucleic Acids Res.* **25**, 3389–3402 (1997). Medline doi:10.1093/nar/25.17.3389

41. E. K. Bomati, M. B. Austin, M. E. Bowman, R. A. Dixon, J. P. Noel, Structural elucidation of chalcone reductase and implications for deoxychalcone biosynthesis. *J. Biol. Chem.* **280**, 30496–30503 (2005). Medline doi:10.1074/jbc.M502239200

42. J. Felsenstein, PHYLIP – Phylogeny inference package (Version 3.2). *Cladistics* **5**, 164 (1989).